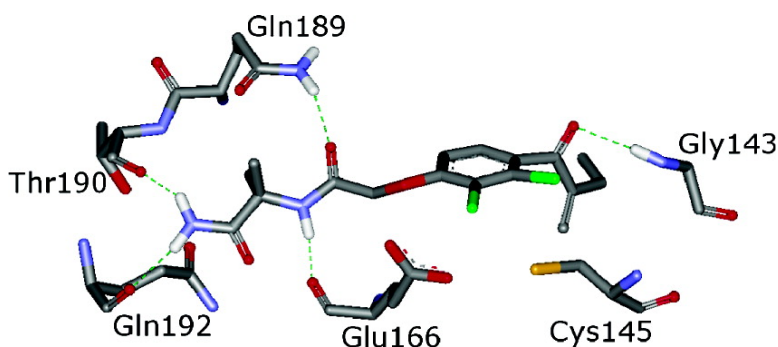


A New Lead for Nonpeptidic Active-Site-Directed Inhibitors of the Severe Acute Respiratory Syndrome Coronavirus Main Protease Discovered by a Combination of Screening and Docking Methods

Ulrich Kaeppler, Nikolaus Stiefl, Markus Schiller, Radim Vicik, Alexander Breuning, Werner Schmitz, Daniel Rupprecht, Carsten Schmuck, Knut Baumann, John Ziebuhr, and Tanja Schirmeister

J. Med. Chem., **2005**, 48 (22), 6832-6842 • DOI: 10.1021/jm0501782 • Publication Date (Web): 01 October 2005

Downloaded from <http://pubs.acs.org> on March 29, 2009



More About This Article

Additional resources and features associated with this article are available within the HTML version:

- Supporting Information
- Links to the 3 articles that cite this article, as of the time of this article download
- Access to high resolution figures
- Links to articles and content related to this article
- Copyright permission to reproduce figures and/or text from this article

[View the Full Text HTML](#)



A New Lead for Nonpeptidic Active-Site-Directed Inhibitors of the Severe Acute Respiratory Syndrome Coronavirus Main Protease Discovered by a Combination of Screening and Docking Methods^{||}

Ulrich Kaeppler,[†] Nikolaus Stiefl,[†] Markus Schiller,[†] Radim Vicik,[†] Alexander Breuning,[†] Werner Schmitz,[‡] Daniel Rupprecht,[§] Carsten Schmuck,[§] Knut Baumann,[†] John Ziebuhr,[#] and Tanja Schirmeister^{*,†}

Institute of Pharmacy and Food Chemistry, University of Würzburg, Am Hubland, D-97074 Würzburg, Germany, Department of Physiological Chemistry II, Theodor-Boveri-Institute, University of Würzburg, Am Hubland, D-97074 Würzburg, Germany, Institute of Organic Chemistry, University of Würzburg, Am Hubland, D-97074 Würzburg, Germany, and Institute of Virology and Immunology, University of Würzburg, Versbacher Strasse 7, D-97078 Würzburg, Germany

Received February 24, 2005

The coronavirus main protease, M^{pro}, is considered to be a major target for drugs suitable for combating coronavirus infections including severe acute respiratory syndrome (SARS). An HPLC-based screening of electrophilic compounds that was performed to identify potential M^{pro} inhibitors revealed etacrynic acid *tert*-butylamide (**6a**) as an effective nonpeptidic inhibitor. Docking studies suggested a binding mode in which the phenyl ring acts as a spacer bridging the inhibitor's activated double bond and its hydrophobic *tert*-butyl moiety. The latter is supposed to fit into the S4 pocket of the target protease. Furthermore, these studies revealed etacrynic acid amide (**6b**) as a promising lead for nonpeptidic active-site-directed M^{pro} inhibitors. In a fluorimetric enzyme assay using a novel fluorescence resonance energy transfer (FRET) pair labeled substrate, compound **6b** showed a K_i value of 35.3 μ M. Since the novel lead compound does not target the S1', S1, and S2 subsites of the enzyme's substrate-binding pockets, there is room for improvement that underlines the lead character of compound **6b**.

Introduction

Coronaviruses are important pathogens that mainly cause respiratory and enteric disease in humans, live-stock, and domestic animals.¹ For example, transmissible gastroenteritis virus (TGEV), a group I coronavirus, causes diarrhea in young piglets,² and SARS-CoV, a group II coronavirus, causes severe acute respiratory syndrome (SARS).^{3–5} It is generally believed that SARS-CoV only very recently crossed the species barrier from an unknown animal reservoir to humans,⁶ thus causing the severe SARS epidemic in 2002–2003 with more than 800 deaths worldwide.⁷ With genome sizes of about 30 kilobases, coronaviruses are the largest plus-strand RNA viruses currently known. In their life cycles, coronaviruses employ several unique mechanisms and enzymes that discriminate them from all other RNA viruses.^{8,9} Following receptor-mediated entry into the host cell, the genome RNA is translated to produce two large replicase polyproteins that are autocatalytically cleaved by two or three viral proteases.¹⁰ The key enzyme in this process is the coronavirus main protease, M^{pro}, a cysteine protease featuring a two- β -barrel fold, which cleaves the replicase polyproteins at as many as 11 conserved sites.^{10–13} Because of its essential role in proteolytic processing, the M^{pro} is considered to be an

attractive target for new antiviral drugs against SARS and other coronavirus infections.¹²

A number of potential inhibitors have been proposed employing molecular modeling and virtual screening techniques.^{14–22} However, the inhibitory potency of these compounds has not yet been verified. Only a small number of potent protease inhibitors were identified by screening assays thus far. These include an HIV protease inhibitor identified by a broad cell-based screening,²³ two nonpeptidic heterocyclic compounds that were identified by a broad protease inhibition screening,²⁴ a 3-quinolinecarboxylic acid ester and an imidazolidine identified by a cell-based assay,²⁵ mercury and zinc containing inhibitors,²⁶ and boronic acid derivatives that are supposed to target serine residues of the protease.²⁷ Most of these studies used commercially available compound libraries for their screening assays. With the exception of a peptidyl chloromethyl ketone¹³ and the peptidomimetic inhibitor AG-7088,^{28,29} none of the compounds identified to date were developed and predicted to target the active site cysteine residue. This lack of active-site-directed lead structures motivated the search for new leads with proven active-site-directed activity.

The scrutinized compounds contain electrophilic building blocks (aziridine, epoxide, Michael system) that are known to react with nucleophilic amino acids within the active site of proteases.^{28,30–32} Derivatives of etacrynic acid (**5a**) (Scheme 1), which is a well-known diuretic drug³³ and which also contains an activated double bond, were chosen as potential nonpeptidic leads owing to their activity toward the cysteine protease papain.³⁴ The properties of these compounds as new nonpeptidic SARS-CoV M^{pro} inhibitors are presented herein.³⁵

^{||} Dedicated to Prof. Dr. Claus Herdeis, Institute of Pharmacy and Food Chemistry, University of Würzburg, on the occasion of his 60th birthday.

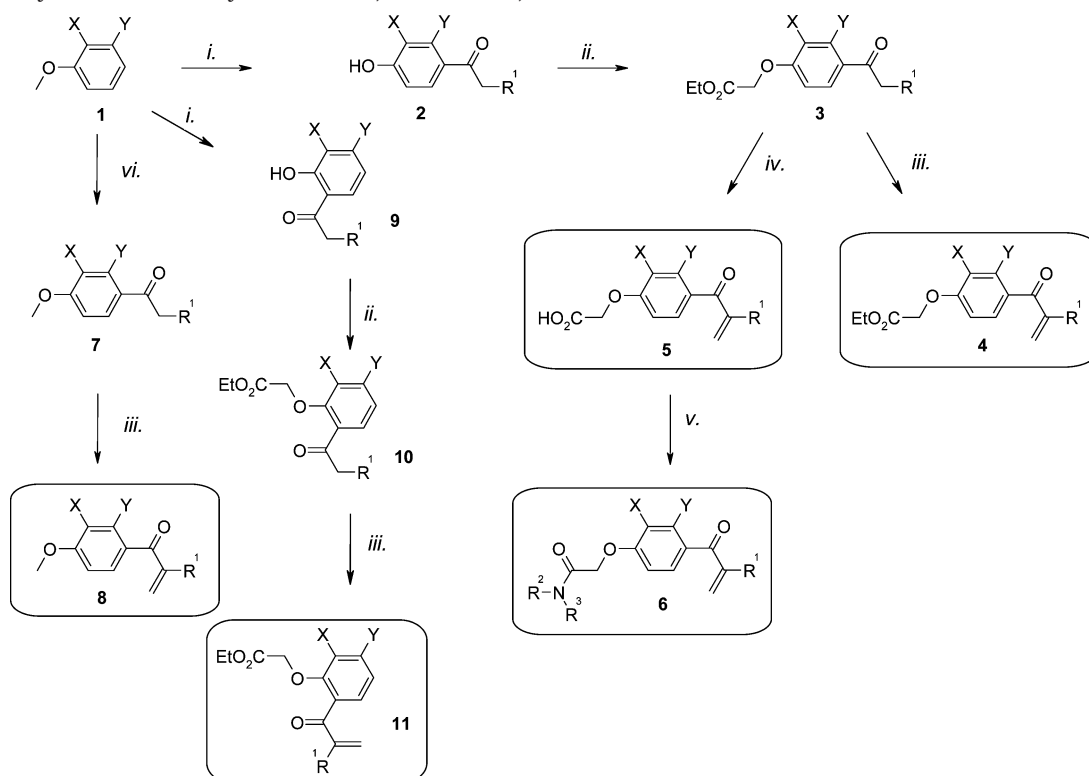
* To whom correspondence should be addressed. Phone: ++49-(0)931-888-5440. Fax: ++49-(0)931-888-5494. E-mail: schirmei@pzc.uni-wuerzburg.de.

[†] Institute of Pharmacy and Food Chemistry.

[‡] Theodor-Boveri-Institute.

[§] Institute of Organic Chemistry.

[#] Institute of Virology and Immunology.

Scheme 1. Synthesis of Etacrynic Acid (**5a**, X = Y = Cl, R¹ = Et) and Derivatives^a

^a (i) 1.5 equiv of R¹-CH₂-C(O)Cl, CH₂Cl₂, 3 equiv of AlCl₃, 3 h, 0°C, 3 h reflux; (ii) Br-CH₂-CO₂Et, *K*-*tert*-butylate, KI, THF; (iii) TMDM, Ac₂O, CHCl₃; (iv) HCHO, EtOH, K₂CO₃; (v) HOSuc, DCC, HN(R²)(R³), CH₂Cl₂; (vi) R¹-CH₂-C(O)Cl, CH₂Cl₂, 1.5 equiv of AlCl₃, 3 h, 0°C.³⁴

Results and Discussion

Syntheses. Etacrynic acid (**5a**) and its analogues and ester derivatives were prepared according to a previously described pathway (Scheme 1, Table 1).³⁴ Anisoles (**1**) (X, Y = H, Cl, CH₃) were acylated with acid chlorides (R¹ = CH₃, C₂H₅) by Friedel-Crafts acylation. Depending on the acylation conditions, the acylated phenols (**2**, **9**) or anisoles (**7**) were obtained. The phenols (**2**, **9**) were alkylated to yield phenoxy acetic acid esters (**3**, **10**). These compounds and the anisoles (**7**) were subjected to the Mannich reaction with TMDM to yield compound series **4**, **8**, and **11**, containing the desired Michael system. Aldol condensation of phenoxy acetic acid esters (**3**) with HCHO yielded the acids (**5**). Aminolysis of the active ester of etacrynic acid (**5a**) gave the amides (**6**).³⁴

Enzyme Inhibition and Docking. First, a comprehensive screening³⁵ was performed with an HPLC-based assay using VSYGSTLQ|AGLRKMA^{36,37} for TGEV M^{pro} and VSVNSTLQ|SGLRKMA^{12,37,38} for SARS-CoV M^{pro} as substrates (Table 2). As the most promising inhibitor, etacrynic acid *tert*-butylamide (**6a**) was identified by the screening (Figure 1, >80% inhibition of both enzymes at 100 μM).

This derivative is one of a series of etacrynic acid amides that were developed as new nonpeptidic cysteine protease inhibitors containing a Michael system as the electrophilic fragment.³⁴ Only the amide **6a** showed inhibition of the coronaviral M^{pro} compounds, whereas the acid **5a** is only weakly active in the HPLC assay (approximately 20% inhibition at 100 μM, Table 2). To better understand the relevant interactions between this inhibitor and the SARS-CoV M^{pro}, docking experiments using FlexX³⁹ were carried out. The binding site

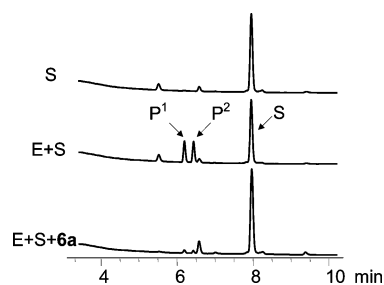


Figure 1. HPLC profiles of proteolytic reactions for determination of enzymatic activity of SARS-CoV M^{pro} and of inhibition by **6a** ([I] = 100 μM): E, enzyme (1.4 μg in a final volume of 30 μL); S, substrate VSVNSTLQ|SGLRKMA, [S] = 0.50 mM; P¹ and P², hydrolysis products. The enzyme was incubated for 30 min with the inhibitor followed by an incubation period of 60 min with the substrate. After the incubation, a 2% TFA solution was added and the mixture was separated on an HPLC system (Zorbax SB-Aq RP-C18 column with a linear gradient from 5% to 90% acetonitrile in water containing 0.1% TFA). Peaks were detected at 215 nm.

was extracted from the recently published structure of an enzyme inhibitor complex¹³ of SARS M^{pro} (PDB code: 1UK4).

In the best docking pose⁴⁰ (Figure 2) compound **6a** is spanning across the binding pockets with the *tert*-butyl group located in the hydrophobic S4 pocket, the dichlorobenzyl moiety located close to S3, and the terminal ethyl group at the Michael system pointing away from the active site (Figure 2). Hydrogen bonds can be formed between the ligand and amino acids His163, Glu166, and Gln189 (Figure 3).⁴¹

The docking suggests that the reactive center of the inhibitor, namely, the activated double bond, is located

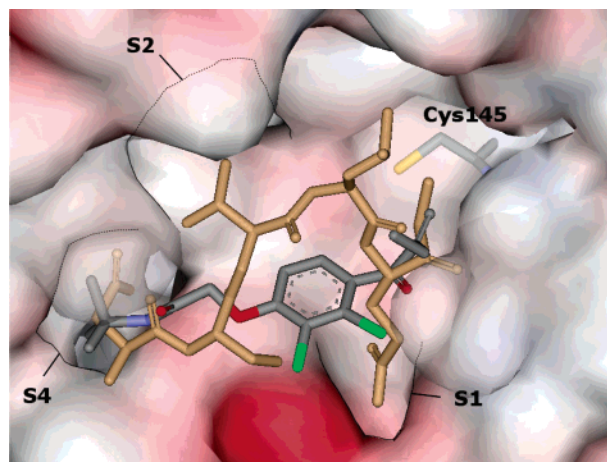


Figure 2. Docking overlay of the hexapeptidyl CMK¹³ (light brown) and the etacrynic acid amide (**6a**) (colored by atom). Compound **6a** is spanning across the binding pockets with the *tert*-butyl group located in the hydrophobic S4 pocket, the dichlorobenzyl moiety located close to S3, and the terminal ethyl group at the Michael system pointing away from the active site.

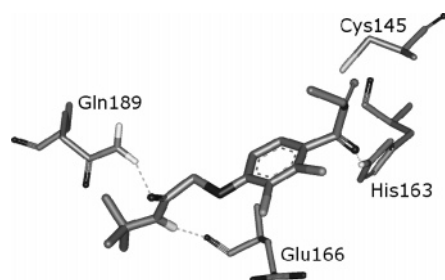


Figure 3. Proposed binding mode of **6a**. Hydrogen bonds are formed between the ligand and amino acids His163, Glu166, and Gln189 of the enzyme. The docking suggests that the reactive center of the inhibitor, namely, the activated double bond, is located in proximity to the sulfur of Cys145, pinpointing that these compound targets the active site.

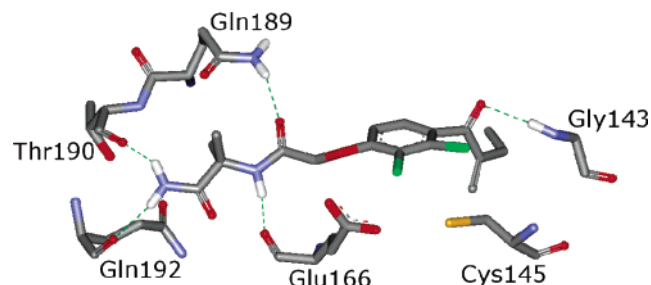


Figure 4. Proposed binding mode of **6b**. This compound is predicted to form hydrogen bonds with Gln189, Glu166, Thr190, and Gln192 via its terminal amino group. The carbonyl group of the Michael system interacts with Gly143. The reactive double bond is still close to the sulfur of Cys145.

in proximity to the sulfur of Cys145 (3.40 Å),⁴² pinpointing that these compounds target the active-site. Next, the S4 pocket was inspected to figure out whether a modification of the *tert*-butyl moiety could enhance affinity. It was deduced from this analysis that the introduction of an additional hydrogen bond donor may increase affinity. Compound **6a** was extended with an α -methyl-alanine amide residue attached to the terminal carboxylic acid to compound **6b** (Table 1). This was done because the latter compound was thought to be able to form an additional hydrogen bond, because it still fits the

Table 1. Etacrynic Acid Derivatives Tested for SARS-CoV M^{pro} Inhibition

compd	R ¹	Y	X	$\begin{matrix} R^2 \\ N \\ R^3 \\ R^4 \end{matrix}$
4a	Et	Cl	Cl	
4b	Me	CH ₃	H	
4c	Et	CH ₃	H	
4d	Me	H	H	
4e	Me	H	Cl	
4f	Et	H	Cl	
5a	Et	Cl	Cl	
5b	Et	CH ₃	CH ₃	
6a	Et	Cl	Cl	NH- <i>tert</i> -butyl
6b	Et	Cl	Cl	NHC(CH ₃) ₂ CONH ₂
6c	Et	Cl	Cl	(<i>S</i>)-AlaOBn
6d	Et	Cl	Cl	(<i>R</i>)-AlaOBn
6e	Et	Cl	Cl	Gly-(<i>S</i>)-PheNH ₂
6f	Et	Cl	Cl	NH- <i>n</i> -butyl
6g	Et	Cl	Cl	
6h	Et	Cl	Cl	
6i	Et	Cl	Cl	NH-phenyl
6k	Et	Cl	Cl	NH- <i>n</i> -hexyl
6l	Et	Cl	Cl	NH-benzyl
8a	Me	H	Cl	
8b	Et	H	Cl	
8c		H	Cl	
11a	Et	Cl	H	

Table 2. Inhibition of TGEV M^{pro} and SARS-CoV M^{pro} by Etacrynic Acid Derivatives As Obtained in the HPLC-Based Assay^a

compd	TGEV M ^{pro}	SARS-CoV M ^{pro}
5a	+	+ (100 μ M)
6a	+++	+++ (100 μ M)
		++ (50 μ M)
		++ (20 μ M)
6b	+++	+++ (100 μ M)
		++ (50 μ M)
		++ (20 μ M)

^a (+) 10–50% inhibition; (++) 50–80% inhibition; (+++) >80% inhibition.

active site and because it was thought to be synthetically accessible. To double-check whether this manually derived modification actually results in an improved interaction, compound **6b** was automatically docked into the enzyme. It was predicted to form the same hydrogen bonds with Gln189 and Glu166 as compound **6a**.⁴³ In addition to that, compound **6b** also has the potential to form two additional hydrogen bonds to Thr190 and Gln192 via its terminal amino group (see Figure 4).⁴⁴

Because of the additional hydrogen bonds, the molecule slightly turns around within the active site so that the carbonyl group of the Michael system is no longer

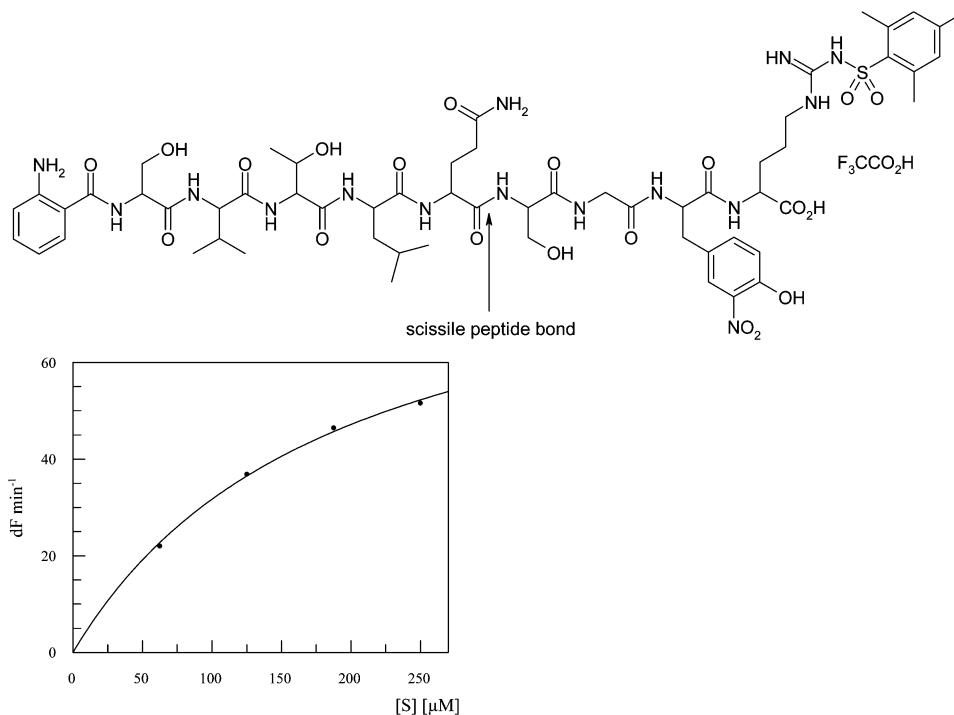


Figure 5. Hydrolysis of the FRET pair labeled substrate *o*-aminobenzoic acid Ser-Val-Thr-Leu-Gln-|-Ser-Gly-(*o*-NO₂)Tyr-Arg-(Mts)-OH by SARS-CoV M^{pro}. For determination of the K_m value, the substrate was used in concentrations between 50 and 300 μ M. Fluorescence increase was measured over a period of 10 min. Values were corrected for the inner filter effect. K_m was determined as $190 \pm 23 \mu$ M, the mean value from three independent assays.

in the proximity of His163 but instead interacts with Gly143. However, the reactive double bond is still close to the sulfur of Cys145 (3.48 Å).⁴² Docking of a few more not yet synthesized compounds with amines and alkyl chains and aliphatic rings of various length and complexity did not result in as good docking scores and as plausible binding modes as those of compound **6b**. Hence, it was decided to synthesize the latter compound to verify the predictions derived from docking.

Compound **6b** was synthesized via aminolysis of the active ester of etacrynic acid with α -methylalanine amide. HPLC assays on SARS-CoV M^{pro} with the above-mentioned peptide substrate showed the inhibitors (**6a** and **6b**) to be equipotent between 20 and 100 μ M (Table 2). Since the HPLC assay is time-consuming and intricate and only allows for crude differentiation between the inhibitors, we performed fluorimetric assays at 100 μ M inhibitor concentrations using a fluorescence resonance energy transfer (FRET) pair labeled substrate. The substrate *o*-aminobenzoic acid Ser-Val-Thr-Leu-Gln-|-Ser-Gly-(*o*-NO₂)Tyr-Arg(Mts)-OH, which was chosen according to previously described assays,^{24,45} was synthesized by automated solid-phase peptide synthesis. In contrast to the substrate described in ref 24, we omitted deprotection of the arginine side chain and used *o*-nitro-Tyr (3-nitro-Tyr)⁴⁵ instead of *m*-nitro-Tyr as the fluorescence acceptor.⁴⁶ These modifications do not decrease the affinity to the enzymes but in contrast enhance it (TGEV M^{pro} $K_m = 85.5 \mu$ M, SARS-CoV M^{pro} $K_m = 190 \mu$ M (Figure 5); the reference value for *o*-aminobenzoic acid Ser-Val-Thr-Leu-Gln-|-Ser-Gly-(*m*-NO₂)Tyr-Arg-OH on SARS-CoV M^{pro} is $K_m = 820 \pm 130 \mu$ M).²⁴

To check the validity of the docking results, we tested several other etacrynic acid derivatives in addition to amide **6b** in the fluorimetric assay (Figures 6 and 7,

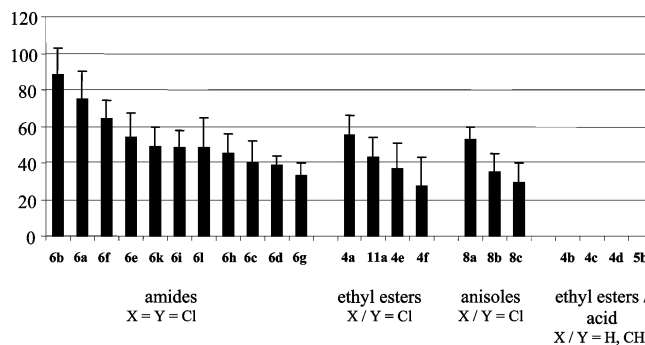


Figure 6. Percent inhibition of SARS-CoV M^{pro} by etacrynic acid derivatives **4–6**, **8**, and **11** as determined in the FRET assay. *o*-Aminobenzoic acid Ser-Val-Thr-Leu-Gln-|-Ser-Gly-(*o*-NO₂)Tyr-Arg(Mts)-OH was used as substrate in a final concentration of 50.0 μ M; the final enzyme concentration was 4.25 μ g mL⁻¹. Inhibitors were used at 100 μ M final concentrations. Fluorescence increase was measured over a period of 20 min. Inhibitors are ranked according to their inhibition potency. For structures of compounds, see Scheme 1 and Table 1.

Table 3). Some of these derivatives have already also been tested on the CAC1 model cysteine protease papain (Table 3).³⁴

Among these derivatives, the most potent SARS-CoV M^{pro} inhibitor is indeed amide **6b** (Figures 6 and 7), which corroborates the predicted binding of the α -methylalanine amide residue into the S4 pocket. In addition, the results clearly show that at least one chloro substituent at the phenyl moiety is necessary for SARS-CoV M^{pro} inhibition (Figure 6). Compounds with an unsubstituted phenyl ring or a methyl substituent (**4b–d**) are inactive at 100 μ M. This also applies to the dimethyl substituted phenoxy acetic acid **5b**. With respect to this latter finding, the inhibition of the coronaviral cysteine protease follows a different trend than the inhibition of papain for which a quite good K_i

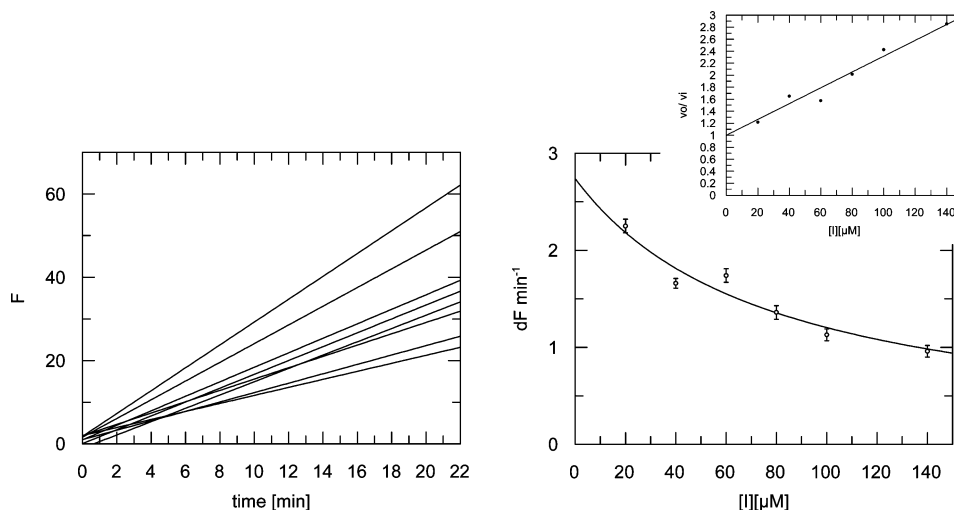


Figure 7. Inhibition of SARS-CoV M^{pro} by **6b**: (left) progress curves at increasing inhibitor concentrations of 0, 10, 20, 40, 60, 80, 100, 140 μM ; (right) nonlinearized and linearized Dixon plot. F is in fluorescence units. *o*-Aminobenzoic acid Ser-Val-Thr-Leu-Gln-|-Ser-Gly-(*o*-NO₂)Tyr-Arg(Mts)-OH was used as substrate in a final concentration of 50.0 μM ; the final enzyme concentration was 4.25 $\mu\text{g mL}^{-1}$. Fluorescence increase was measured over a period of 20 min.

Table 3. Comparison of Inhibition of SARS-CoV M^{pro} and Papain³⁴ by Etacrynic Acid Derivatives **4–6**

compd	SARS-CoV M ^{pro} % inhibition at 100 μM ^{a,b}	SARS-CoV M ^{pro} K_i [μM] ^b	papain K_i [μM] ^c
4a	55	nd ^d	13.0
4d	ni ^c	nd ^d	1960
5a	20	nd ^d	375
5b	ni ^c	nd ^d	33
6a	75	45.8 \pm 3.2	3.2
6b	88	35.3 \pm 3.0	nd ^d
6e	54	nd ^d	188
6f	64	nd ^d	6.2
6g	33	nd ^d	413
6h	45	nd ^d	204

^a Values corresponding to Figure 6. ^b For details see Experimental Section. ^c Taken from ref 34. ^c ni: no inhibition. ^d nd: not determined.

value of 33 μM was obtained for **5b** (Table 3).³⁴ In contrast to this, the other derivatives listed in Table 3 exhibit the same order of inhibition potency for SARS-CoV M^{pro} and for papain.

Concerning the possible diuretic activity of etacrynic acid derivatives, it is quite promising that only the amides and esters display SARS-CoV M^{pro} inhibition. Diuretic activity of etacrynic acid is connected to the free acid group because of active transport of the drug to its site of diuretic action (the luminal membrane of the cells of the thick ascending loop) via the organic acid transport mechanism.^{47,48} Thus, hydrolytically stable amides or esters should be void of diuretic side effects.

Summary

A comprehensive HPLC-based screening with various protease inhibitors containing electrophilic moieties revealed nonpeptidic etacrynic acid *tert*-butyl amide (**6a**) as the most promising lead for new inhibitors of coronaviral main proteases. Docking experiments with **6a** and other etacrynic acid amides led to the development of **6b**, which exhibits slightly improved affinity to SARS-CoV M^{pro}. To the best of our knowledge, this compound is the first nonpeptidic inhibitor targeting the active site cysteine residue of the SARS-CoV M^{pro}. Recently and independently of our work a paper concerning the development of inhibitors derived from AG-7088 was

published.⁶³ According to the predicted binding mode, the phenyl moiety of the etacrynic acid derivatives serves as a spacer that links the active site and the S4 pocket. The fact that there are no interactions with other subsites known to contribute to the M^{pro} substrate binding (S1', S1, and S2) might explain the not yet optimal inhibitory potency (**6b**: $K_i = 35.3 \mu\text{M}$) and the missing selectivity of this inhibitor class. Interactions with these binding sites could be achieved with additional substituents attached to the phenyl ring that might lead to superior activity and improved selectivity compared to CAC1 proteases. Our future efforts will therefore concentrate on variations of the substituents at the phenyl ring of **6b**.

Experimental Section

General Information. Melting points were determined in open capillary on a melting point apparatus, model 530, from Büchi, Switzerland. CHN analyses were determined with a CHNS-932, Leco. HR-EI mass spectra were recorded on a Finnigan MAT 90, Thermo Electron GmbH, Germany, at 70 eV ionization energy. HR-ESI-MS spectra were recorded on a FT-ICR APEX II from Bruker, Germany. ESI mass spectra were recorded on an Agilent 1100 ion trap equipped with an HPLC system from Agilent. NMR spectra were recorded on an AVANCE 400 MHz spectrometer from Bruker Biospin GmbH, Germany (solvent, CDCl₃. ¹H NMR, 400.13 MHz; ¹³C NMR, 100.61 MHz). IR spectra were recorded on a PharmalyzIR FT-IR spectrometer from BioRad. The α values were determined on a 241 polarimeter from Perkin-Elmer. The refractive indices were determined on an apparatus from ATG GmbH, Germany. Hydrostatic column chromatography was performed with silica gel from Merck (silica gel 60, 0.063–0.2 mm or 70–230 mesh).

All solvents were purified and dried prior to use according to standard literature procedures.

Protein Expression and Purification. The TGEV M^{pro} was expressed in *Escherichia coli* and purified to near homogeneity using amylose agarose (New England Biolabs), phenyl Sepharose HP (Pharmacia), and Superdex 75 (Pharmacia) columns using previously described protocols.^{11,36} The purified enzyme was stored at -70°C in buffer containing 12 mM Tris-HCl, pH 7.4, 120 mM NaCl, 0.1 mM EDTA, and 1 mM DTT. To express the SARS-CoV M^{pro}, the coding sequence of amino acid residues from 3236 to 3544 of SARS-CoV (strain Frankfurt 1) polyprotein **1a** was amplified by RT-PCR from poly(A) RNA isolated from SARS-CoV-infected Vero E6 cells⁴⁹ using oligo-

nucleotides JZ468 (5'-TCTGCTGTTCTGCAGAGTGGTTTTAG-GAAATGGCATTCC-3') and JZ429N (5'-AAAGAATTCTTAAT-GTGATGTGTATGTGTGTAACACCAGAGCATTTGTCTAA CAACATC-3'). The PCR product was 5'-phosphorylated using T4 polynucleotide kinase, digested with EcoRI and ligated with XmnI/EcoRI-digested pMal-c2 plasmid DNA (New England Biolabs). The resultant plasmid, pMal-SARS-CoV-M^{pro}-His, encoded the *E. coli* maltose-binding protein (MBP) fused to the SARS-CoV M^{pro} (residues 1–304). At the MBP–M^{pro} junction, the plasmid encoded five amino acid residues, SAVLQ, that precede the SARS-CoV M^{pro} sequence in the viral replicase polyprotein. This N-terminal extension of the M^{pro} sequence reconstituted the natural N-terminal M^{pro} autoproteolytic site (SAVLQ|SGFRK) and thus resulted in a very efficient intracellular autocatalytic release of the M^{pro}'s N-terminus (H₂N–SGFRK...) from the MBP fusion protein. This generated the authentic M^{pro} N-terminus, which is known to be required for the full enzymatic activities of coronavirus main proteases.^{11,12} At its C-terminus, the M^{pro} domain was extended by six consecutive His residues, allowing for affinity chromatography purification of the protein on Ni-NTA agarose columns. The pMal-SARS-CoV-M^{pro}-His plasmid DNA was used to transform competent *E. coli* TB1 cells. Following induction of expression with 1 mM isopropyl β -D-thiogalactopyranoside, the cells were grown at 25 °C for 3 h. Cell lysates were prepared as described previously,³⁶ and the His-tagged SARS-CoV M^{pro} was purified on Ni-NTA agarose (Qiagen) and Superdex 75 (Pharmacia) columns. The purified protein was concentrated using Centricon YM-3 filter units (Millipore) and stored at –70 °C in buffer containing 15 mM Tris-HCl, pH 8.0, 200 mM NaCl, 0.1 mM EDTA, and 1 mM DTT.

HPLC Assays. The peptide substrate VSYGSLQAGL-RKMA was purchased from Jerini, Berlin, Germany, and VSVNSTLQSGLRKMA was purchased from Bachem. The assays were performed using a 20 mM Tris-HCl buffer at pH 7.5 containing 15% DMSO (final concentration), 200 mM NaCl, 1 mM DTT, and 1 mM EDTA. An amount of 1.4 μ g of enzyme (TGEV M^{pro} or SARS-CoV M^{pro}), either 0.44 mM VSYGSLQ|AGLRKMA³⁶ as substrate for TGEV M^{pro} or 0.50 mM VSVNSTLQ|SGLRKMA^{12,37,38} as substrate for SARS-CoV M^{pro} and 20, 50, or 100 μ M inhibitor were used in a final volume of 30 μ L.³⁶ Stock solutions of substrates and inhibitors were prepared in DMSO and diluted with assay buffer, and enzymes were dissolved in buffer. The enzymes were incubated 30 min with each inhibitor followed by an incubation period with the respective substrate for 30 min (TGEV M^{pro}) or 60 min (SARS-CoV M^{pro}). After the incubation, a 2% TFA solution was added and the mixture was separated on a Varian ProStar HPLC system using an Agilent Zorbax SB-Aq RP-C18 column with a linear gradient from 5% to 90% acetonitrile in water (flow: 1 mL min⁻¹) containing 0.1% TFA. Peaks were detected at 215 nm. Calculations of inhibition were performed by comparing the peak integrals of the two hydrolysis products (P¹ and P², Figure 1) and the substrate peak integrals (S, Figure 1) relative to the corresponding signal areas in the absence of inhibitor. All assays were done in triplicate.

Fluorimetric Enzyme Assays. The fluorimetric enzyme assays were performed on a Cary Eclipse fluorescence spectrophotometer from Varian, Darmstadt, Germany, using a microplate reader (excitation 325 nm, emission 425 nm). For the inhibition assays 96-well microplates from Nunc GmbH, Wiesbaden, Germany, were used. Assays were performed at 25 °C in a 20 mM Tris-HCl buffer, pH 7.5, containing 0.1 mM EDTA, 1 mM DTT, 200 mM NaCl, and 12.5% DMSO (final concentration) in a total volume of 200 μ L. The final substrate concentration for inhibition assays was 50 μ M, and the final enzyme concentration was 4.25 μ g mL⁻¹. Inhibitors were used at 100 μ M final concentration for preliminary screening (results shown in Figure 6) or at concentrations between 10 and 140 μ M for determination of *K_i* values (results shown in Figure 7 and Table 3).

For determination of *K_m* values, the substrate was used in concentrations between 50 and 300 μ M (SARS-CoV M^{pro}) and

between 20 and 100 μ M (TGEV M^{pro}). Values were corrected for the inner filter effect according to refs 24 and 50.

Fluorescence increase was measured over a period of 10 min for *K_m* determination and 20 min for inhibition assays. Substrate and inhibitor stock solutions were prepared in DMSO and were diluted with assay buffer, and enzymes were dissolved in buffer.

K_m and *K_i*⁵¹ values were calculated by nonlinear regression analyses using the program GraFit.⁵² All values are mean values from at least three independent assays.

Synthesis of the FRET Pair Labeled Substrate. The substrate was synthesized by solid-phase peptide synthesis on a Milligen 9050 PepSynthesizer using standard Fmoc protocol. Synthesis was performed in DMF/DCM (60:40) with DIC/HOBt activation starting from Fmoc-Arg(Mts)-Wang-resin. The substrate was cleaved from the resin by treatment with TFA/DCM (1:1). The product substrate as TFA salt was purified and characterized by HPLC (see Supporting Information) and LC–MS. ESI-MS calcd for C₅₉H₈₅N₁₅O₂₀S, [M – H]⁺: 1357.48. Found: 1357.0.

Syntheses of Inhibitors. The syntheses of compounds 4a,d, 5a,b, 6a,c,f–h,k are described in ref 34.

General Methods for Syntheses of Etacrynic Acid Derivatives 4b,c,e,f, 8a–c, and 11a.

Method A: Friedel–Crafts Acylation to Compounds 2 and 9. Amounts of 1 equiv of anisole and 1.5 equiv of acid chloride are dissolved under N₂ atmosphere in 50–100 mL of absolute CH₂Cl₂, and the mixture is cooled to 0–5 °C. An amount of 1.5 equiv of AlCl₃ is added within 30 min, and the mixture is stirred for 2–3 h. A total of 75–100 mL of CH₂Cl₂ is removed by distillation and is substituted by the same amount of CH₂Cl₂. This procedure is repeated twice. An additional amount of 1.5 equiv of AlCl₃ is added, and the mixture is heated under reflux for 2.5–3 h. The mixture is poured on ice and acidified with concentrated HCl to pH 1. Tartaric acid is added for the complexation of aluminum until the solution is cleared up. The solution is extracted with EtOEt, and the organic layer is washed with water and KOH solution (10%). The organic layer is dried with Na₂SO₄, filtered off, and the crude product obtained after removal of the solvent is recrystallized.

Method B: Syntheses of Phenoxyacetic Acid Esters (3). An amount of 1 equiv of phenol is dissolved in THF under N₂ atmosphere. Then 1 equiv of *K-tert*-butylate and a catalytic amount (0.1 equiv) of KI are added. The mixture is heated at 60 °C, and an amount of 1.1–2.0 equiv of ethyl bromoacetate is added slowly. The mixture is stirred for 30–60 min, poured into water, acidified to pH 1 with concentrated HCl, and extracted with EtOEt. The organic layer is washed with 10% KOH, water, and brine and dried with Na₂SO₄. After filtration, the solvent is removed in vacuo and the remaining residue is recrystallized or distilled.

Method C: Mannich Reaction with TMDM To Produce 4. Amounts of 1 equiv of phenoxy acetic acid ester derivative, 20 equiv of TMDM, and 20 equiv of Ac₂O are mixed. The mixture is heated under reflux at 85 °C. The reaction is followed by ¹H NMR spectroscopy. After completion of the reaction, the mixture is dissolved in 200 mL of CHCl₃. Saturated K₂CO₃ solution is added until gas evolution stops. The mixture is filtered through Celite, and the filtrate is dried with Na₂SO₄. After filtration, the solvent is removed in vacuo. The product is purified by column chromatography.

The syntheses of etacrynic acid amides 6b, 6d, 6e, 6i,⁵³ and 6l were performed starting from etacrynic acid (5a) and the corresponding amines as described earlier.³⁴

Ethyl [3-Methyl-4-(2-methylacryloyl)phenoxy]acetate (4b). Synthesis of Ethyl (3-Methyl-4-propionylphenoxy)acetate (3b). Method B is used. Starting from 13.7 g (83.4 mmol) of 1-(4-hydroxy-2-methylphenyl)propane-1-one (2b),⁵⁴ 9.23 g (84 mmol) *K-tert*-butylate, and 20.9 g (125.1 mmol) of ethyl bromoacetate in 75 mL of THF, an amount of 10.75 g (43.0 mmol, 52%) of ethyl-(3-methyl-4-propionylphenoxy)acetate (3b) is obtained as a colorless solid; mp 33–34 °C (ethanol). Anal. (C₁₄H₁₈O₄) C, H, N. ¹H NMR (400.13 MHz,

CDCl₃, 300 K, TMS): δ 1.18 (3H, t, J = 7.33 Hz, H₃C-CH₂-O), 1.30 (3H, t, J = 7.07 Hz, H₃C-CH₂-C), 2.53 (3H, s, Ar-CH₃), 2.90 (2H, q, J = 7.33 Hz, H₃C-CH₂-O-), 4.28 (2H, q, J = 7.07 Hz, H₃C-CH₂-C), 4.65 (2H, s, -O-CH₂-), 6.75 (2H, m, arom H₂ + H₆), 7.70 (1H, d, J = 8.34 Hz, arom H₅). ¹³C NMR (100.61 MHz, CDCl₃, 300 K, TMS): δ 8.59 (CH₃-CH₂-CO), 14.17 (O-CH₂-CH₃), 22.27 (Ar-CH₃), 34.01 (CH₃-CH₂-CO), 61.53 (O-CH₂-CH₃), 65.13 (O-CH₂-CO), 111.09 (arom C₂ or C₆, CH), 118.10 (arom C₂ or C₆, CH), 131.22 (arom qC₃), 132.16 (arom C₅, CH), 141.82 (arom qC₄), 159.70 (arom qC₁), 168.42 (O-CH₂-CO), 202.74 (Ar-CO).

Synthesis of Ethyl [3-Methyl-4-(2-methylacryloyl)phenoxy]acetate (4b). Method C is used. Starting from 1.31 g (5 mmol) of ethyl (3-methyl-4-propionylphenoxy)acetate (**3b**), 1.40 g (13.6 mmol) of TMDM, and 5.4 g (52.5 mmol) of acetic anhydride, an amount of 179 mg (14%) of **4b** is obtained as a colorless liquid after purification by column chromatography on silica gel 60 (cyclohexane/ethyl acetate 10/1). n_D^{22} = 1.5240. HR-EI-MS (70 eV, m/z , [M]⁺) calcd for C₁₅H₁₈O₄: 262.1200. Found: 262.1201. ¹H NMR (400.13 MHz, CDCl₃, 300 K, TMS): δ 1.30 (3H, t, J = 7.07 Hz, CH₂-CH₃), 2.03 (3H, s, H₃C-C=CH₂), 2.33 (3H, s, Ar-CH₃), 4.28 (2H, q, J = 7.07 Hz, -CH₂-CH₃), 4.64 (2H, s, O-CH₂-CO-), 5.54 (1H, s, =CH₂), 5.90 (1H, s, =CH₂), 6.70 (1H, dd, J = 2.40 Hz, J = 8.48 Hz, arom H₆), 6.77 (1H, d, J = 2.40 Hz, arom H₂), 7.27 (1H, d, J = 8.48 Hz, arom H₅). ¹³C NMR (100.61 MHz, CDCl₃, 300 K): δ 14.18 (O-CH₂-CH₃), 17.68 (H₃C-C=CH₂), 20.32 (Ar-CH₃), 61.47 (O-CH₂-CH₃), 65.26 (O-CH₂-CO), 100.63 (arom C₆, CH), 117.26 (arom C₂, CH), 128.57 (=CH₂), 130.64 (arom C₅, CH), 132.23 (arom qC₄), 139.47 (H₃C-C=CH₂), 145.42 (arom qC₁), 158.95 (O-CH₂-CO), 168.59 (Ar-CO-).

Ethyl [3-Methyl-4-(2-methylenebutyryl)phenoxy]acetate (4c). **Synthesis of Ethyl (4-Butyryl-3-methylphenoxy)acetate (3c).** Method B is used. Starting from 8.02 g (45 mmol) 1-(4-hydroxy-2-methylphenyl)butane-1-one (**2c**),⁵⁵ 5.05 g (45 mmol) of *K-tert*-butylate, 8.26 g (49.5 mmol) of ethyl bromoacetate, an amount of 9.2 g (34.8 mmol, 77%) of ethyl (4-butyryl-3-methylphenoxy)acetate (**3c**) is obtained as colorless liquid. n_D^{22} = 1.5200. Anal. (C₁₅H₂₀O₄) C, H, N. ¹H NMR (400.13 MHz, CDCl₃, 300 K, TMS): δ 0.97 (3H, t, J = 7.33 Hz, H₃C-CH₂-CH₂), 1.30 (3H, t, J = 7.08 Hz, H₃C-CH₂-O), 1.72 (2H, sext, J = 7.33 Hz, H₃C-CH₂-CH₂), 2.52 (3H, s, Ar-CH₃), 2.84 (2H, t, J = 7.33 Hz, H₃C-CH₂-CH₂), 4.28 (2H, q, J = 7.08 Hz, H₃C-CH₂-O), 4.65 (2H, s, O-CH₂-CO), 6.73-6.76 (2H, m, arom H₂ + H₆), 7.69 (1H, d, J = 8.34 Hz, arom H₅). ¹³C NMR (100.61 MHz, CDCl₃, 300 K): δ 13.77 (H₃C-CH₂-CH₂), 14.06 (H₃C-CH₂-O), 17.98 (H₃C-CH₂-CH₂), 22.05 (Ar-CH₃), 42.81 (H₃C-CH₂-CH₂), 61.40 (H₃C-CH₂-O), 65.01 (O-CH₂-CO), 110.97 (arom C₂, CH), 117.98 (arom C₆, CH), 131.16 (arom C₅, CH), 131.32 (arom qC₄), 141.60 (arom qC₃, C-CH₃), 159.58 (arom qC₁), 168.32 (O-CH₂-CO), 202.38 (Ar-CO).

Synthesis of Ethyl [3-Methyl-4-(2-methylenebutyryl)phenoxy]acetate (4c). Method C is used. Starting from 1.38 g (5 mmol) of ethyl (4-butyryl-3-methylphenoxy)acetate (**3c**), 1.40 g (13.6 mmol) of TMDM, and 5.4 g (52.5 mmol) of acetic anhydride and after purification by column chromatography on silica gel 60 (cyclohexane/ethyl acetate 9/1), an amount of 390 mg (1.4 mmol, 28%) of **4c** is obtained as a colorless liquid. n_D^{22} = 1.5243. HR-EI-MS (70 eV, m/z , [M]⁺) calcd for C₁₆H₂₀O₄: 276.1362. Found: 276.1357. ¹H NMR (400.13 MHz, CDCl₃, 300 K, TMS): δ 1.13 (3H, t, J = 7.46 Hz, H₃C-CH₂), 1.31 (3H, t, J = 7.07 Hz, H₃C-CH₂-O), 2.34 (3H, s, Ar-CH₃), 2.46 (2H, q, J = 7.46 Hz, H₃C-CH₂), 4.28 (2H, q, J = 7.07 Hz, H₃C-CH₂-O), 4.64 (2H, s, O-CH₂-CO), 5.53 (1H, s, =CH), 5.82 (1H, s, =CH), 6.70 (1H, dd, J = 2.53 Hz, J = 8.71 Hz, arom H₆), 6.77 (1H, d, J = 2.53 Hz, arom H₂), 7.28 (1H, d, J = 8.71 Hz, arom H₅). ¹³C NMR (100.61 MHz, CDCl₃, 300 K): δ 12.51 (H₃C-CH₂), 14.15 (H₃C-CH₂-O), 20.38 (Ar-CH₃), 24.17 (H₃C-CH₂), 61.46 (H₃C-CH₂-O), 65.23 (O-CH₂-CO), 110.62 (arom C₆, CH), 117.20 (arom C₂, CH), 126.23 (=CH₂), 130.87 (arom C₅, CH), 132.47 (arom qC₄), 139.64 (arom qC₃, C-CH₃), 151.33 (qC=CH₂), 158.98 (arom qC₁), 168.56 (O-CH₂-CO), 199.61 (Ar-CO).

Ethyl [2-Chloro-4-(2-methylacryloyl)phenoxy]acetate (4e). **Synthesis of Ethyl (2-Chloro-4-propionylphenoxy)acetate (3e).** Method B is used. Starting from 13.85 g (75 mmol) of 1-(3-chloro-4-hydroxyphenyl)propane-1-one (**2e**),⁵⁶ 8.42 g (75 mmol) of *K-tert*-butylate, and 18.78 g (122.5 mmol) of ethyl bromoacetate in 75 mL of THF, an amount of 13.0 g (48.02 mmol, 64%) of ethyl (2-chloro-4-propionylphenoxy)acetate (**3e**) is obtained as a colorless solid, mp 125-126.5 °C (ethanol). Anal. (C₁₃H₁₅ClO₄) C, H, N. ¹H NMR (400.13 MHz, CDCl₃, 300 K, TMS): δ 1.20 (3H, t, J = 7.33 Hz, H₃C-CH₂-CO), 1.29 (3H, t, J = 7.20 Hz, H₃C-CH₂-O), 2.93 (2H, q, J = 7.33 Hz, H₃C-CH₂-CO), 4.27 (2H, q, J = 7.20 Hz, H₃C-CH₂-O), 4.76 (2H, s, O-CH₂-CO), 6.84 (1H, d, J = 8.58 Hz, arom H₆), 7.83 (1H, dd, J = 2.02 Hz, J = 8.59 Hz, arom H₅), 8.02 (1H, d, J = 2.02 Hz, arom H₃). ¹³C NMR (100.61 MHz, CDCl₃, 300 K, TMS): δ 8.23 (H₃C-CH₂-CO), 14.13 (H₃C-CH₂-O), 31.55 (H₃C-CH₂-CO), 61.74 (H₃C-CH₂-O), 65.96 (O-CH₂-CO), 112.52 (arom C₆, CH), 123.49 (arom qC₄ or qC₂-Cl), 128.03 (arom C₅, CH), 130.73 (arom C₃, CH), 131.51 (arom qC₄ or qC₂-Cl), 156.96 (arom qC₁), 167.70 (O-CH₂-CO), 198.32 (Ar-CO).

Synthesis of Ethyl [2-Chloro-4-(2-methylacryloyl)phenoxy]acetate (4e). Method C is used. Starting from 1.35 g (5 mmol) of ethyl (2-chloro-4-propionylphenoxy)acetate (**3e**), 766 mg (7.5 mmol) of TMDM, and 5.4 g (52.5 mmol) of acetic anhydride, an amount of 225 mg (0.8 mmol, 16%) of **4e** was obtained as a colorless solid, mp 55-56 °C (cyclohexane). Anal. (C₁₄H₁₅ClO₄) C, H, N. ¹H NMR (400.13 MHz, CDCl₃, 300 K, TMS): δ 1.30 (3H, t, J = 7.16 Hz, -CH₂-CH₃), 2.05 (3H, s, CH₃), 4.29 (2H, q, J = 7.16 Hz, -CH₂-CH₃), 4.77 (2H, s, O-CH₂-), 5.57 (1H, s, =C-H), 5.87 (1H, s, =C-H), 6.84 (1H, d, J = 8.53 Hz, Ar-H), 7.66 (1H, dd, J = 2.15 Hz, J = 8.83 Hz, Ar-H), 7.85 (1H, d, J = 2.15 Hz, Ar-H). ¹³C NMR (100.61 MHz, CDCl₃, 300 K): δ 14.12 (-CH₂-CH₃), 18.81 (-CH₃), 61.70 (-CH₂-CH₃), 65.97 (-O-CH₂-), 112.37 (arom C₆, CH), 123.13 (arom C_{2/4}, q), 125.99 (=CH₂), 129.59 (arom C₅, CH), 131.74 (arom qC_{2/4}), 132.12 (arom C₃, CH), 143.46 (H₂C=C), 156.56 (arom qC₁), 167.73 (-CH₂-CO-O-), 195.76 (-CO-Ar).

Ethyl [2-Chloro-4-(2-methylenebutyryl)phenoxy]acetate (4f). **Synthesis of Ethyl (4-Butyryl-2-chlorophenoxy)acetate (3f).** Method B is used. Starting from 9.93 g (50 mmol) of 1-(3-chloro-4-hydroxyphenyl)butane-1-one (**2f**),⁵⁷ 5.61 g (50 mmol) of *K-tert*-butylate, 9.18 g (55 mmol) of ethyl bromoacetate in 75 mL of THF, an amount of 10.37 g (36.42 mmol, 73%) of the target compound is obtained as colorless solid, mp 97-98 °C (ethanol). Anal. (C₁₄H₁₇ClO₄) C, H, N. ¹H NMR (400.13 MHz, CDCl₃, 300 K, TMS): δ 1.00 (3H, t, J = 7.46 Hz, H₃C-CH₂-CH₂), 1.30 (3H, t, J = 7.20 Hz, H₃C-CH₂-O), 1.75 (2H, sext, J = 7.33 Hz, 7.46 Hz, H₃C-CH₂-CH₂), 2.88 (2H, t, J = 7.33 Hz, H₃C-CH₂-CH₂), 4.28 (2H, q, J = 7.20 Hz, H₃C-CH₂-O), 4.77 (2H, s, O-CH₂-CO), 6.84 (1H, d, J = 8.59 Hz, arom H₆), 7.83 (1H, dd, J = 2.27 Hz, J = 8.59 Hz, arom H₅), 8.02 (1H, d, J = 2.27 Hz, arom H₃). ¹³C NMR (100.61 MHz, CDCl₃, 300 K, TMS): δ 13.86 (H₃C-CH₂-CH₂), 14.14 (H₃C-CH₂-O), 17.79 (H₃C-CH₂-CH₂), 40.25 (H₃C-CH₂-CH₂), 61.74 (H₃C-CH₂-O), 65.97 (O-CH₂-CO), 112.52 (arom C₆, CH), 123.49 (arom qC₄), 128.11 (arom C₅, CH), 130.80 (arom C₃, CH), 131.71 (arom qC₂, C-Cl), 156.96 (arom qC₁), 167.71 (O-CH₂-CO), 197.88 (Ar-CO).

Synthesis of Ethyl [2-Chloro-4-(2-methylenebutyryl)phenoxy]acetate (4f). Method C is used. Starting from 2.85 g (10 mmol) of ethyl-(4-butyryl-2-chlorophenoxy)acetate (**3f**) 9.53 g (93.23 mmol) of TMDM, and 10.8 g (105.8 mmol) of acetic anhydride, an amount of 990 mg (3.34 mmol, 33%) of **4f** is obtained as a colorless liquid. n_D^{22} = 1.5398. Anal. (C₁₅H₁₇ClO₄) C, H, N. ¹H NMR (400.13 MHz, CDCl₃, 300 K, TMS): δ 1.11 (3H, t, J = 7.45 Hz, H₃C-CH₂), 1.30 (3H, t, J = 7.08 Hz, O-CH₂-CH₃), 2.46 (2H, q, J = 7.45 Hz, H₃C-CH₂), 4.28 (2H, q, J = 7.08 Hz, O-CH₂-CH₃), 4.77 (2H, s, O-CH₂-CO), 5.52 (1H, s, =CH), 5.78 (1H, s, =CH), 6.84 (1H, d, J = 8.59 Hz, arom H₆), 7.68 (1H, dd, J = 2.27 Hz, J = 8.59 Hz, arom H₅), 7.87 (1H, d, J = 2.27 Hz, arom H₃). ¹³C NMR (100.61 MHz, CDCl₃, 300 K): δ 12.28 (H₃C-CH₂-C=), 14.09 (O-CH₂-CH₃),

25.42 ($H_3C-CH_2-C=$), 61.69 ($O-CH_2-CH_3$), 65.94 ($O-CH_2-CO$), 112.33 (arom C_6 , CH), 123.13 ($C=CH_2$ + arom qC_2 , C-Cl), 129.64 (arom C_5 , CH), 132.02 (arom qC_4), 132.13 (arom C_3 , CH), 149.38 ($C=CH_2$), 156.64 (arom qC_1), 167.71 ($O-CH_2-C=O$), 195.98 (Ar-C=O).

2-{2-[2,3-Dichloro-4-(2-methylenebutyryl)phenoxy]acetyl-amino}-2-methylpropionic Acid Carboxamide (6b). Colorless solid, mp 157–158 °C (ethyl acetate). Anal. ($C_{17}H_{20}Cl_2N_2O_4$) C, H, N. 1H NMR (400.13 MHz, $CDCl_3$, 300 K, TMS): δ 1.15 (3H, t, $J = 7.47$ Hz, H_3C-CH_2), 1.67 (6H, s, $O-(CH_3)_2$), 2.47 (2H, q, $J = 7.47$ Hz, H_3C-CH_2), 4.54 (2H, s, $O-CH_2-CO-$), 5.58 (1H, s, $C=CH_2$), 5.63 (1H, s, $CO-NH_2$), 5.95 (1H, s, $C=CH_2$), 6.44 (1H, s, $CO-NH_2$), 6.87 (1H, d, $J = 8.49$ Hz, arom H_6), 7.19 (1H, d, $J = 8.49$ Hz, arom H_5), 7.45 (1H, s, $CO-NH-$). ^{13}C NMR (100.61 MHz, $CDCl_3$, 300 K, TMS): δ 12.38 (H_3C-CH_2), 23.40 (H_3C-CH_2), 25.16 ($C-(CH_3)_2$), 57.25 ($qC-(CH_3)_2$), 68.24 ($O-CH_2-CO$), 110.90 (arom C_6 , CH), 123.04 (arom qC_2 , C-Cl or qC_4), 127.16 (arom C_5 , CH), 128.73 ($=CH_2$), 131.54 (arom qC_3 , C-Cl), 134.28 (arom qC_2 , C-Cl or qC_4), 150.17 ($qC=CH_2$), 154.37 (arom qC_1), 166.59 ($O-CH_2-CO$), 176.08 ($CO-NH_2$), 195.53 (Ar-CO).

The amine used for coupling with etacrylic acid (**5a**), namely, 2-amino-2-methylpropionic acid carboxamide HCl (α -methylalaninecarboxamide HCl), was synthesized according to ref 58.

(R)-Benzyl 2-{2-[2,3-Dichloro-4-(2-methylenebutyryl)phenoxy]acetyl-amino}propionate (6d). Yellowish liquid; $\alpha^{25}_D + 11.95^\circ$ (methanol, c 2.18). Anal. ($C_{23}H_{23}Cl_2NO_5$) C, H, N. HR-EI-MS (70 eV, m/z , $[M - Cl]^+$) calcd for $C_{23}H_{23}Cl_2NO_5$: 428.1259. Found: 428.1261. 1H NMR (400.13 MHz, $CDCl_3$, 300 K, TMS): δ 1.15 (3H, t, $J = 7.33$ Hz, H_3C-CH_2), 1.51 (3H, d, $J = 7.33$ Hz, Ala- CH_3), 2.48 (2H, q, $J = 7.33$ Hz, H_3C-CH_2), 4.58 (dd, $J = 2.02$ Hz, $J = 14.40$ Hz, $O-CH_2-CO-NH$), 4.73 (1H, q, $J = 7.07$ Hz, $J = 7.33$ Hz, Ala- CH), 5.21 (dd, $J = 2.28$ Hz, $J = 12.25$ Hz, benzyl- CH_2), 5.58 (1H, s, $C=CH_2$), 5.95 (1H, s, $C=CH_2$), 6.85 (1H, d, $J = 8.46$ Hz, arom H_6), 7.17 (1H, d, $J = 8.46$ Hz, arom H_5), 7.34–7.40 (6H, m, benzyl- CH , NH). ^{13}C NMR (100.61 MHz, $CDCl_3$, 300 K): δ 12.40 (H_3C-CH_2), 18.39 (Ala- CH_3), 23.42 (H_3C-CH_2), 48.02 (Ala- CH), 67.26 (benzyl- CH_2), 68.18 ($O-CH_2-CO-NH$), 110.96 (arom C_6 , CH), 123.71 (arom qC_3 , C-Cl or arom qC_4), 127.13 (arom C_5 , CH), 128.21 (arom benzyl- CH), 128.55 (arom benzyl- CH), 128.67 ($qC-CH_2$), 131.54 (arom qC_3 , C-Cl or arom qC_4), 134.29 (arom qC_2 , C-Cl), 135.17 (arom qC_1 , benzyl), 150.21 ($qC=CH_2$), 154.53 (arom qC_1), 166.31 ($O-CH_2-CO-NH$), 172.02 (Ala-CO), 195.54 (Ar-CO).

(S)-2-(2-{2-[2,3-Dichloro-4-(2-methylenebutyryl)phenoxy]acetyl-amino}acetyl-amino)-3-phenylpropionamide (6e). Colorless solid; $\alpha^{25}_D + 7.27^\circ$ (methanol, c 1.10); mp 146–148 °C (methanol). HR-ESI-MS (m/z , $[M + H]^+$) calcd for $C_{24}H_{25}Cl_2N_3O_5$: 506.1250. Found: 506.1258. 1H NMR (400.13 MHz, $DMSO-d_6$, 300 K): δ 1.07 (3H, t, $J = 7.33$ Hz, H_3C-CH_2), 2.36 (2H, q, $J = 7.33$ Hz, H_3C-CH_2), 2.76 (1H, m, $J = 13.64$ Hz, Phe- CH_2), 3.02 (1H, m, $J = 13.64$ Hz, Phe- CH_2), 3.67 (1H, dd, $J = 5.56$ Hz, $J = 16.65$ Hz, Gly- CH_2), 3.83 (1H, dd, $J = 5.56$ Hz, $J = 16.65$ Hz, Gly- CH_2), 4.44 (1H, m, $J = 4.30$ Hz, $J = 4.80$ Hz, Phe- CH), 4.75 (2H, s, $O-CH_2-CO$), 7.09 (1H, s, Phe- NH_2), 7.12 (1H, d, $J = 8.59$ Hz, arom H_6), 7.14–7.26 (5H, m, arom H (Phe)), 7.30 (1H, d, $J = 8.59$ Hz, arom H_5), 7.43 (1H, s, Phe- NH_2), 8.11 (1H, d, $J = 5.56$ Hz, Gly- NH), 8.14 (1H, d, $J = 8.34$ Hz, Phe- NH). ^{13}C NMR (100.61 MHz, $DMSO-d_6$, 300 K): δ 12.32 (H_3C-CH_2), 22.89 (H_3C-CH_2), 37.54 (Phe- CH_2), 41.67 (Gly- CH_2), 53.78 (Phe- CH), 67.75 ($O-CH_2-CO$), 112.04 (arom C_6 , CH), 121.09 (arom qC_4), 126.19 (arom C_4 , Phe- CH), 127.48 (arom C_5 , CH), 128.01 (arom Phe- CH), 129.08 (arom Phe- CH), 129.30 (arom qC_3 , C-Cl), 129.40 ($C=CH_2$), 132.53 (arom qC_2 , C-Cl), 137.91 (arom qC_1), 149.30 ($qC=CH_2$), 155.28 (arom qC_1), 166.86 ($O-CH_2-CO$), 168.00 (Gly-CO), 172.75 (Phe-CO), 195.07 (Ar-CO).

2-[2,3-Dichloro-4-(2-methylenebutyryl)phenoxy]-N-phenylacetamide (6i). Colorless solid, mp 125–126 °C (cyclohexane/ethyl acetate) [ref 53, 145–147 °C]. HR-EI-MS (70 eV, m/z , $[M]^+$) calcd for $C_{19}H_{17}Cl_2NO_3$: 377.0580. Found: 377.0580.

1H NMR (400.13 MHz, $CDCl_3$, 300 K, TMS): δ 1.16 (3H, t, $J = 7.33$ Hz, H_3C-CH_2), 2.48 (2H, q, $J = 7.33$ Hz, H_3C-CH_2), 4.70 (2H, s, $O-CH_2-CO$), 5.60 (1H, s, $C=CH_2$), 5.97 (1H, s, $C=CH_2$), 6.93 (1H, d, $J = 8.34$ Hz, arom H_6), 7.18 (1H, t, $J = 7.58$ Hz, arom H_4 , anilide), 7.22 (1H, d, $J = 8.34$ Hz, arom H_5), 7.39 (2H, t, $J = 7.58$ Hz, arom H_3 + arom H_5 , anilide), 7.62 (2H, d, $J = 7.58$ Hz, arom H_2 + arom H_6 , anilide), 8.53 (1H, s, NH). ^{13}C NMR (100.61 MHz, $CDCl_3$, 300 K): δ 12.40 (H_3C-CH_2), 23.42 (H_3C-CH_2), 68.38 ($O-CH_2-CO$), 111.20 (arom C_6 , CH), 120.01 (arom C_2 + C_6 , CH, anilide), 123.07 (arom qC_4), 125.11 (arom C_4 , CH, anilide), 127.33 (arom C_5 , CH), 128.79 ($qC=CH_2$), 129.21 (arom C_3 + C_5 , CH, anilide), 131.64 (arom qC_3 , C-Cl), 134.60 (arom qC_2 , C-Cl), 136.71 (arom qC_1 , anilide), 150.22 ($qC=CH_2$), 154.31 (arom qC_1), 164.56 ($O-CH_2-CO$), 195.43 (Ar-CO).

N-Benzyl-2-[2,3-dichloro-4-(2-methylenebutyryl)phenoxy]acetamide (6l). Colorless solid, mp 90–92 °C (cyclohexane). Anal. ($C_{20}H_{19}Cl_2NO_3$) C, H, N. 1H NMR (400.13 MHz, $CDCl_3$, 300 K, TMS): δ 1.15 (3H, t, $J = 7.46$ Hz, H_3C-CH_2), 2.47 (2H, q, $J = 7.46$ Hz, H_3C-CH_2), 4.58 (2H, d, $J = 6.07$ Hz, benzyl- CH_2), 4.63 (2H, s, $O-CH_2-CO$), 5.57 (1H, s, $C=CH_2$), 5.95 (1H, s, $C=CH_2$), 6.87 (1H, d, $J = 8.47$ Hz, arom H_6), 7.07 (1H, s, NH), 7.18 (1H, d, $J = 8.47$ Hz, arom H_5), 7.28–7.38 (5H, m, arom H benzyl residue). ^{13}C NMR (100.61 MHz, $CDCl_3$, 300 K): δ 12.38 (H_3C-CH_2), 23.40 (H_3C-CH_2), 43.13 (benzyl- CH_2), 68.32 ($-O-CH_2-CO$), 110.97 (arom C_6 , CH), 123.00 (arom qC_4), 127.18 (arom C_5 , CH), 127.54 (arom benzyl- CH), 127.72 (arom benzyl- CH), 128.66 ($qC=CH_2$), 128.82 (arom benzyl- CH), 131.50 (arom qC_3 , C-Cl), 134.27 (arom qC_2 , C-Cl), 137.46 (arom benzyl- qC_1), 150.19 ($qC=CH_2$), 154.48 (arom qC_1), 166.61 ($O-CH_2-CO$), 195.46 (Ar-CO).

1-(3-Chloro-4-methoxyphenyl)-2-methylpropenone (8a). Method C is used. Starting from 1.98 g (10 mmol) of 1-(3-chloro-4-methoxyphenyl)propane-1-one (**7a**),⁵⁹ 11.42 g (112 mmol) of TMDM, and 16.2 g (158 mmol) of acetic anhydride, the crude product obtained is purified by column chromatography on silica gel 60 (cyclohexane/ethyl acetate 19/1). Yield 433 mg (2.1 mmol, 21%), colorless solid, mp 49–50 °C (cyclohexane/ethyl acetate). HR-EI-MS (70 eV, m/z , $[M]^+$) calcd for $C_{11}H_{11}ClO_2$: 210.0442. Found: 210.0441. 1H NMR (400.13 MHz, $CDCl_3$, 300 K, TMS): δ 2.06 (3H, s, CH_3), 3.97 (3H, s, $O-CH_3$), 5.56 (1H, s, $C=CH_2$), 5.85 (1H, s, $C=CH_2$), 6.96 (1H, d, $J = 8.59$ Hz, arom H_6), 7.72 (1H, dd, $J = 2.02$ Hz, $J = 8.59$ Hz, arom H_5), 7.85 (1H, d, $J = 2.02$ Hz, arom H_3). ^{13}C NMR (100.63 MHz, $CDCl_3$, 300 K): δ 18.91 (CH_3), 56.34 ($O-CH_3$), 111.08 (arom C_5 , CH), 122.47 (arom qC_4), 125.54 ($qC=CH_2$), 129.98 (arom C_6 , CH), 130.66 (arom qC_2 , C-Cl), 131.81 (arom C_3 , CH), 143.56 ($qC=CH_2$), 158.22 (arom qC_1), 195.92 (Ar-CO).

1-(3-Chloro-4-methoxyphenyl)-2-methylenebutane-1-one (8b). Method C is used. Starting from 2.13 g (10 mmol) of 1-(3-chloro-4-methoxyphenyl)butane-1-one (**7b**),⁵⁷ 9.21 g (90 mmol) of TMDM, and 16.2 g (158 mmol) of acetic anhydride, the crude product obtained is purified by column chromatography. Yield 941 mg (4.19 mmol, 42%), colorless liquid. $n_D^{22} = 1.5620$. HR-EI-MS (70 eV, m/z , $[M]^+$) calcd for $C_{12}H_{13}ClO_2$: 224.0599. Found: 224.0596. 1H NMR (400.13 MHz, $CDCl_3$, 300 K, TMS): δ 1.12 (3H, t, $J = 7.33$ Hz, CH_2-CH_3), 2.47 (2H, q, $J = 7.33$ Hz, CH_2-CH_3), 3.97 (3H, s, $O-CH_3$), 5.51 (1H, s, = CH), 5.76 (1H, s, = CH), 6.96 (1H, d, $J = 8.58$ Hz, arom H_5), 7.73 (1H, dd, $J = 2.02$ Hz, $J = 8.58$ Hz, arom H_6), 7.86 (1H, d, $J = 2.02$ Hz, arom H_3). ^{13}C NMR (100.63 MHz, $CDCl_3$, 300 K, TMS): 12.33 (H_3C-CH_2), 25.56 (H_3C-CH_2), 56.37 ($O-CH_3$), 111.11 (arom C_5 , CH), 122.52 (arom qC_1), 122.71 ($=CH_2$), 130.08 (arom C_6 , CH), 131.00 (arom qC_3 , C-Cl), 131.85 (arom C_2 , CH), 149.51 ($C=CH_2$, q), 158.34 (arom qC_4), 196.20 (Ar-CO).

1-(3-Chloro-4-methoxyphenyl)-2-methylene-4-(4-nitrophenyl)butane-1-one (8c). Synthesis of 1-(3-Chloro-4-methoxyphenyl)-4-(4-nitrophenyl)butane-1-one (**7c**). Method A is used. Starting from 1.90 g (13.3 mmol) of 2-chloro anisole (**1c**), 4.89 g (21.5 mmol) of 4-(4-nitrophenyl)butyryl chloride,⁶⁰ and 2×2.66 g (2×20 mmol) of $AlCl_3$ in 50 mL of CH_2Cl_2 , an amount of 4.09 g (12.25 mmol, 92%) of the desired compound

is obtained as yellow crystals after purification by column chromatography, mp 84–85 °C (ethanol). Anal. (C₁₇H₁₆ClNO₄) C, H, N. ¹H NMR (400.13 MHz, CDCl₃, 300 K, TMS): δ 2.11 (2H, quin, *J* = 7.71 Hz, *J* = 7.08 Hz, -CH₂-CH₂-CO-), 2.82 (2H, t, *J* = 7.71 Hz, CH₂-CH₂-CH₂-CO), 2.94 (2H, t, *J* = 7.08 Hz, -CH₂-CO), 3.97 (3H, s, O-CH₃), 6.96 (1H, d, *J* = 8.79 Hz, arom H₅), 7.37 (2H, d, *J* = 8.72 Hz, arom H₆ + H₆'), 7.84 (1H, dd, *J* = 2.09 Hz, *J* = 8.79 Hz, arom H₆'), 7.96 (1H, d, *J* = 2.09 Hz, arom H₂), 8.16 (2H, d, *J* = 8.72 Hz, arom H₃ + H₃'), 13C NMR (100.61 MHz, CDCl₃, 300 K): δ 25.13 (-CH₂-CH₂-CO), 35.00 (-CH₂-CH₂-CH₂-CO), 36.98 (-CH₂-CO), 56.37 (O-CH₃), 111.31 (arom C₅, CH), 122.92 (arom C₃, C-Cl), 123.71 (arom C₃ + C₅, CH), 128.35 (arom C₆, CH), 129.24 (arom C₂ + C₆, CH), 130.31 (arom C₂, CH), 130.39 (arom qC₁), 146.50 (arom qC₄'), 149.54 (arom qC₁'), 158.80 (arom qC₄), 196.94 (C=O).

Synthesis of 1-(3-Chloro-4-methoxyphenyl)-2-methylene-4-(4-nitrophenyl)butane-1-one (8c). Method C is used. Starting from 1.67 g (5 mmol) of 1-(3-chloro-4-methoxyphenyl)-4-(4-nitrophenyl)butane-1-one (7c), 4.46 g (40.9 mmol) of TMDM, and 5.4 g (52.9 mmol) of acetic anhydride, the crude product 8c was purified by column chromatography on silica gel 60 (CHCl₃). Yield 789 mg (2.28 mmol, 46%), yellow crystals, mp 86–87 °C (CHCl₃). HR-EI-MS (70 eV, *m/z*, [M]⁺) calcd for C₁₈H₁₆ClNO₄: 345.0762. Found: 345.0769. ¹H NMR (400.13 MHz, CDCl₃, 300 K, TMS): δ 2.82 (2H, t, *J* = 7.64 Hz, Ar-CH₂-CH₂-), 2.95 (2H, t, *J* = 7.64 Hz, Ar-CH₂-CH₂-), 3.98 (3H, s, O-CH₃), 5.58 (1H, s, =CH₂), 5.76 (1H, s, =CH₂), 6.95 (1H, d, *J* = 8.59 Hz, arom H₅), 7.35 (2H, d, *J* = 8.72 Hz, arom H₂' + H₆'), 7.65 (1H, dd, *J* = 2.27, *J* = 8.59 Hz, arom H₆'), 7.78 (1H, d, *J* = 2.27 Hz, arom H₂), 8.15 (2H, d, *J* = 8.72 Hz, arom H₃' + H₅'). ¹³C NMR (100.61 MHz, CDCl₃, 300 K): δ 33.87 (Ar-CH₂-CH₂), 34.19 (Ar-CH₂-CH₂), 56.38 (O-CH₃), 111.12 (arom C₆, CH), 122.61 (arom qC₂, C-Cl), 123.67 (arom C₃' + C₅', CH), 125.70 (=CH₂), 129.37 (arom C₂' + C₆', CH), 130.02 (arom C₅, CH), 130.50 (arom qC₄'), 131.85 (arom C₃, CH), 146.07 (qC=CH₂), 146.54 (arom qC₄'), 148.98 (arom qC₁'), 158.52 (arom qC₁'), 195.26 (Ar-CO).

Ethyl [5-Chloro-2-(2-methylenebutyryl)phenoxy]acetate (11a). **Synthesis of Ethyl (2-Butyryl-5-chlorophenoxy)acetate (10a).** Method B is used. Starting from 9.48 g (47.7 mmol) of 1-(4-chloro-2-hydroxyphenyl)butane-1-one (9a),⁶¹ 8.35 g (50 mmol) of ethyl bromoacetate, and 5.35 g (47.7 mmol) of *K*-*tert*-butylate in 75 mL of THF, an amount of 9.62 g (33.79 mmol, 71%) of ethyl (2-butyryl-5-chlorophenoxy)acetate (10a) is obtained as a colorless solid, mp 51–52 °C (ethanol). Anal. (C₁₄H₁₇ClO₄) C, H, N. ¹H NMR (400.13 MHz, CDCl₃, 300 K, TMS): δ 0.96 (3H, t, *J* = 7.46 Hz, H₃C-CH₂-CH₂), 1.32 (3H, t, *J* = 7.20 Hz, H₃C-CH₂), 1.71 (2H, sext, *J* = 7.46 Hz, H₃C-CH₂-CH₂), 3.04 (2H, t, *J* = 7.20 Hz, H₃C-CH₂-CH₂), 4.30 (2H, q, *J* = 7.20 Hz, H₃C-CH₂), 4.70 (2H, s, O-CH₂-CO), 6.81 (1H, d, *J* = 1.77 Hz, arom H₂), 7.03 (1H, dd, *J* = 1.77 Hz, *J* = 8.34 Hz, arom H₄'), 7.66 (1H, d, *J* = 8.34 Hz, arom H₅'), ¹³C NMR (100.61 MHz, CDCl₃, 300 K, TMS): δ 13.86 (H₃C-CH₂-CH₂), 14.16 (H₃C-CH₂-O), 17.73 (H₃C-CH₂-CH₂), 45.80 (H₃C-CH₂-CH₂), 61.71 (H₃C-CH₂-O), 65.71 (O-CH₂-CO), 112.89 (arom C₆, CH), 122.12 (arom C₄, CH), 127.62 (arom qC₅, C-Cl), 131.79 (arom C₃, CH), 138.77 (arom qC₂'), 156.99 (arom qC₁'), 167.58 (O-CH₂-C=O), 201.40 (Ar-C=O).

Synthesis of Ethyl [5-Chloro-2-(2-methylenebutyryl)phenoxy]acetate (11a). Method C is used. Starting from 2.85 g (10 mmol) of ethyl (2-butyryl-5-chlorophenoxy)acetate (10a), 19.75 g (193.3 mmol) of TMDM, and 16.2 g (158.7 mmol) of acetic anhydride, the crude product obtained is purified by column chromatography on silica gel 60 (cyclohexane/ethyl acetate). Yield 2.0 g (6.75 mmol, 68%), colorless solid, mp 25–26 °C (cyclohexane/ethyl acetate). Anal. (C₁₅H₁₇ClO₄) C, H, N. ¹H NMR (400.13 MHz, CDCl₃, 300 K, TMS): δ 1.12 (3H, t, *J* = 7.46 Hz, H₃C-CH₂), 1.28 (3H, t, *J* = 7.20 Hz, H₃C-CH₂-O), 2.45 (2H, q, *J* = 7.46 Hz, H₃C-CH₂), 4.25 (2H, q, *J* = 7.20 Hz, H₃C-CH₂-O), 4.59 (2H, s, O-CH₂-CO), 5.67 (1H, s, C=CH₂), 5.87 (1H, s, C=CH₂), 6.81 (1H, d, *J* = 1.77 Hz, arom H₂), 7.03 (1H, dd, *J* = 1.77 Hz, *J* = 8.08 Hz, arom H₄'), 7.21 (1H, d, *J* = 8.08 Hz, arom H₅'), ¹³C NMR (100.63 MHz, CDCl₃,

300 K): δ 12.41 (H₃C-CH₂), 14.09 (H₃C-CH₂-O), 23.51 (H₃C-CH₂), 61.48 (H₃C-CH₂-O), 65.91 (O-CH₂-CO), 113.22 (arom C₂, CH), 121.66 (arom C₄, CH), 127.13 (qC=CH₂), 128.65 (arom qC₆), 130.13 (arom C₅, CH), 136.60 (arom qC₃, C-Cl), 150.70 (qC=CH₂), 155.90 (arom qC₁'), 167.86 (O-CH₂-CO), 196.91 (Ar-CO).

Enzyme Preparation for Docking Procedure. The starting conformation for the docking procedure was the crystal structure of the SARS-CoV M^{pro} in complex with Cbz-Val-Asn-Ser-Thr-Leu-Gln-CMK (PDB code: 1UK4).¹³ Owing to the covalent binding mode of the cocrystallized ligand Cbz-Val-Asn-Ser-Thr-Leu-Gln-CMK, the active center of SARS-CoV M^{pro} as found in the crystal structure is very tight. Hence, prior to docking, the covalent bond between ligand and receptor was eliminated, the ligands' chloromethyl ketone substructure was rebuilt, and water molecules were deleted. Then the enzyme was relaxed using SYBYL 6.9 (hot region around the ligand, 6 Å; interesting region, 12 Å; 5000 steps; Tripos force field).⁶² Since the water molecule in subpocket S2 (HOH16) is deeply buried, the relaxation was also done with this water molecule kept in place. However, no obvious differences in the resulting geometries were observed in both structures. Put differently, for both enzyme conformations, this part of S2 is without reach for a potential ligand; therefore, the conformation obtained with all water molecules deleted was used for docking.

Active Site Definition. Using the SETREF directive within FlexX, the active site was defined as the complete amino acids found within 8 Å of the heavy atoms of the cocrystallized ligand. For interpretation purposes, only those docking poses located within this active site were considered.

Ligand Preparation. All compounds were sketched in 2D and then converted to 3D structures using SYBYL 6.9. Since FlexX is working in torsional space only (i.e., bond lengths and angles are kept constant), a geometry optimization of the ligands (500 steps, Gasteiger-Hueckel charges, dielectric constant of 4.0, Tripos force field) was performed.

Docking Procedure. FlexX was used with standard settings. Base fragment selection was done automatically, and for base fragment placement, the triangle matching strategy was applied. For each ligand, a maximum of 100 placements were stored; however, only those placements where the ligand was positioned within the active site were inspected in detail.

Acknowledgment. Financial support of this work by the DFG (Deutsche Forschungsgemeinschaft) (Grants DFG SCHI 441/3-1, SCHI 441/4-1, and SFB 630, TP A4 to T.S.) (Grant DFG ZI 618/3-1 to J.Z.) (Grant SFB 630, TP C5 to K.B.) (Grants DFG SCHM 1501/6-1 and SFB 630, TP A3 to C.S.) is gratefully acknowledged. We thank Sonja Bayer for excellent technical assistance. We also thank Josef Scheiber for his kind assistance in preparing Figures 2–4.

Appendix

Abbreviations. Amino acids are (*S*)-configured unless otherwise indicated; either the one- or the three-letter code is used. AG-7088, (*E*)-(*S*)-4-[(2*R*,5*S*)-2-(4-fluorobenzyl)-6-methyl-5-[(5-methylisoxazole-3-carbonyl)amino]-4-oxoheptanoylamino]-5-((*S*)-2-oxopyrrolidin-3-yl)pent-2-enoic acid ethyl ester; DCC, dicyclohexylcarbodiimide; CMK, chloromethyl ketone; DCM, dichloromethane; DIC, 1,3-diisopropylcarbodiimide; DMF, dimethylformamide; DMSO, dimethyl sulfoxide; DPPA, diphenylphosphorazidate; DTT, dithiothreitol; EDTA, ethylenediaminetetraacetic acid; EEDQ, 1-ethoxycarbonyl-2-ethoxy-1,2-dihydroquinoline; FRET, fluorescence resonance energy transfer; HOBT, 1-hydroxybenzotriazole; HOSuc, *N*-hydroxysuccinimide; M^{pro}, main protease; Mts, 2,4,6-trimethylbenzenesulfonyl (mesitylenesulfonyl); SARS-CoV, severe acute respiratory syn-

drome coronavirus; TEA, triethylamine; TFA, trifluoroacetic acid' TGEV, transmissible gastroenteritis virus; THF, tetrahydrofurane; TMDM, *N,N,N',N'*-tetramethyldiaminomethane.

Supporting Information Available: IR data and data confirming the purity of the target compounds (HPLC, HRMS, combustion analyses). This material is available free of charge via the Internet at <http://pubs.acs.org>.

References

- Siddell, S. G.; Ziebuhr, J.; Snijder, E. J. Coronaviruses, toroviruses, and arteriviruses. In *Topley and Wilson's Microbiology and Microbial Infections*, 10th ed.; Mahy, B. W. J., ter Meulen, V., Eds.; Virology, Vol. 1.; Hodder Arnold: London, 2005; pp 823–856.
- Enjuanes, L.; van der Zeijst, B. A. M. Molecular basis of transmissible gastroenteritis virus epidemiology. In *The Coronaviridae*; Siddell, S. G., Ed.; Plenum Press: New York, 1995; pp 337–376.
- Drosten, C.; Günther, S.; Preiser, W.; van der Werf, S.; Brodt, H. R.; Becker, S.; Rabenau, H.; Panning, M.; Kolesnikova, L.; Fouchier, R. A.; Berger, A.; Burguiere, A. M.; Cinatl, J.; Eickmann, M.; Escriou, N.; Grywna, K.; Kramme, S.; Manuguerra, J. C.; Müller, S.; Rickerts, V.; Stürmer, M.; Vieth, S.; Klenk, H. D.; Osterhaus, A. D.; Schmitz, H.; Doerr, H. W. Identification of a novel coronavirus in patients with severe acute respiratory syndrome. *N. Engl. J. Med.* **2003**, *348*, 1967–1976.
- Ksiazek, T. G.; Erdman, D.; Goldsmith, C. S.; Zaki, S. R.; Peret, T.; Emery, S.; Tong, S.; Urbani, C.; Comer, J. A.; Lim, W.; Rollin, P. E.; Dowell, S. F.; Ling, A. E.; Humphrey, C. D.; Shieh, W. J.; Guarner, J.; Paddock, C. D.; Rota, P.; Fields, B.; DeRisi, J.; Yang, J. Y.; Cox, N.; Hughes, J. M.; LeDuc, J. W.; Bellini, W. J.; Anderson, L. J. A novel coronavirus associated with severe acute respiratory syndrome. *N. Engl. J. Med.* **2003**, *348*, 1953–1966.
- Peiris, J. S.; Lai, S. T.; Poon, L. L.; Guan, Y.; Yam, L. Y.; Lim, W.; Nicholls, J.; Yee, W. K.; Yan, W. W.; Cheung, M. T.; Cheng, V. C.; Chan, K. H.; Tsang, D. N.; Yung, R. W.; Ng, T. K.; Yuen, K. Y. Coronavirus as a possible cause of severe acute respiratory syndrome. *Lancet* **2003**, *361*, 1319–1325.
- Guan, Y.; Zheng, B. J.; He, Y. Q.; Liu, X. L.; Zhuang, Z. X.; Cheung, C. L.; Luo, S. W.; Li, P. H.; Zhang, L. J.; Guan, Y. J.; Butt, K. M.; Wong, K. L.; Chan, K. W.; Lim, W.; Shorridge, K. F.; Yuen, K. Y.; Peiris, Y. S.; Poon, L. L. Isolation and characterization of viruses related to the SARS coronavirus from animals in southern China. *Science* **2003**, *302*, 276–278.
- Peiris, J. S.; Yuen, K. Y.; Osterhaus, K. D.; Stöhr, K. The severe acute respiratory syndrome. *N. Engl. J. Med.* **2003**, *349*, 2431–2441.
- Ziebuhr, J. Molecular biology of severe acute respiratory syndrome coronavirus. *Curr. Opin. Microbiol.* **2004**, *7*, 412–419.
- Ziebuhr, J. The coronavirus replicase. *Curr. Top. Microbiol. Immunol.* **2005**, *287*, 57–94.
- Ziebuhr, J.; Snijder, E. J.; Gorbalenya, A. E. Virus-encoded proteinases and proteolytic processing in the Nidovirales. *J. Gen. Virol.* **2000**, *81*, 853–879.
- Anand, K.; Palm, G. J.; Mesters, J. R.; Siddell, S. G.; Ziebuhr, J.; Hilgenfeld, R. Structure of coronavirus main proteinase reveals combination of chymotrypsin fold with an extra alpha-helical domain. *EMBO J.* **2002**, *21*, 3213–3224.
- Anand, K.; Ziebuhr, J.; Wadhvani, P.; Mesters, J. R.; Hilgenfeld, R. Coronavirus main proteinase (3CL^{pro}) structure: basis for design of anti-SARS drugs. *Science* **2003**, *300*, 1763–1767.
- Yang, H.; Yang, M.; Ding, Y.; Liu, Y.; Lou, Z.; Zhou, Z.; Sun, L.; Mo, L.; Ye, S.; Pang, H.; Gao, G. F.; Anand, K.; Bartlam, M.; Hilgenfeld, R.; Rao, Z. The crystal structures of severe acute respiratory syndrome virus main protease and its complex with an inhibitor. *Proc. Natl. Acad. Sci. U.S.A.* **2003**, *100*, 13190–13195.
- Liu, B.; Zhou, J. SARS-CoV protease inhibitors design using virtual screening method from natural products libraries. *J. Comput. Chem.* **2005**, *26*, 484–490.
- Rajnarayanan, R. V.; Dakshanamurthy, S.; Pattabiraman, N. "Teaching old drugs to kill new bugs": structure-based discovery of anti-SARS drugs. *Biochem. Biophys. Res. Commun.* **2004**, *321*, 370–378.
- Chou, K.-C.; Wei, D.-Q.; Zhong, W.-Z. Binding mechanism of coronavirus main proteinase with ligands and its implication to drug design against SARS. *Biochem. Biophys. Res. Commun.* **2003**, *308*, 148–151.
- Jenwitheesuk, E.; Samudrala, R. Identifying inhibitors of the SARS coronavirus proteinase. *Bioorg. Med. Chem. Lett.* **2003**, *13*, 3989–3992.
- Zhang, X. W.; Yap, Y. L.; Altmeyer, R. M. Generation of predictive pharmacophore model for SARS-coronavirus main proteinase. *Eur. J. Med. Chem.* **2005**, *40*, 57–62.
- Du, Q.; Wang, S.; Wei, D.; Sirois, S.; Chou, K.-C. Molecular modeling and chemical modification for finding peptide inhibitor against severe acute respiratory syndrome coronavirus main proteinase. *Anal. Biochem.* **2005**, *337*, 262–270.
- Xiong, B.; Gui, C.-S.; Xu, X.-Y.; Luo, C.; Chen, J.; Luo, H.-B.; Chen, L.-L.; Li, G.-W.; Sun, T.; Yu, C.-Y.; Yue, L.-D.; Duan, W.-H.; Shen, J.-K.; Qin, L.; Li, Y.-X.; Chen, K.-X.; Luo, X.-M.; Shen, X.; Shen, J.-H.; Jiang, H.-L. A 3D model of SARS-CoV 3CL proteinase and its inhibitors design by virtual screening. *Acta Pharm. Sin.* **2003**, *24*, 497–504.
- Zhang, X.-W.; Yap, Y. L. Old drugs as lead compounds for a new disease? Binding analysis of SARS coronavirus main proteinase with HIC, psychotic and parasitic drugs. *Bioorg. Med. Chem.* **2004**, *12*, 2517–2521.
- Toney, J. H.; Navas-Martin, S.; Weiss, S. R.; Koeller, A. Sabadinine: A potential non-peptide anti-severe acute-respiratory-syndrome agent identified using structure-aided design. *J. Med. Chem.* **2004**, *47*, 1079–1080.
- Wu, C. Y.; Jan, J. T.; Ma, S. H.; Kuo, C. J.; Juan, H. F.; Cheng, Y. S.; Hsu, H. H.; Huang, H. C.; Wu, D.; Brik, A.; Liang, F. S.; Liu, R. S.; Fang, J. M.; Chen, S. T.; Liang, P. H.; Wong, C. H. Small molecule targeting severe acute respiratory syndrome human coronavirus. *Proc. Nat. Acad. Sci. U.S.A.* **2004**, *101*, 10012–10017.
- Blanchard, J. E.; Elowe, N. H.; Huitema, C.; Fortin, P. D.; Cechetto, J. D.; Eltis, L. D.; Brown, E. D. High-throughput screening identifies inhibitors of the SARS coronavirus main proteinase. *Chem. Biol.* **2004**, *11*, 1445–1453.
- Kao, R. Y.; To, A. P. C.; Ng, L. W. Y.; Tsui, W. H. W.; Lee, T. S. W.; Tsoi, H.-W.; Yuen, K.-Y. Characterization of SARS-CoV main protease and identification of biologically active small molecule inhibitors using a continuous fluorescence-based assay. *FEBS Lett.* **2004**, *576*, 325–330.
- Hsu, J. T.-A.; Kuo, J.-C.; Hsieh, H.-P.; Wang, Y.-C.; Huang, K.-K.; Lin, C. P.-C.; Huang, P.-F.; Chen, X.; Liang, P.-H. Evaluation of metal-conjugated compounds as inhibitors of 3CL protease of SARS-CoV. *FEBS Lett.* **2004**, *574*, 116–120.
- Bacha, U.; Barrila, J.; Velazquez-Campoy, A.; Leavitt, S. A.; Freire, E. Identification of novel inhibitors of the SARS coronavirus main protease 3CL^{pro}. *Biochemistry* **2004**, *43*, 4906–4912.
- Matthews, D. A.; Dragovich, P. S.; Webber, S. E.; Fuhrman, S. A.; Patick, A. K.; Zalman, S. L.; Hendrickson, T. F.; Love, R. A.; Prins, T. J.; Marakovits, J. T.; Zhou, R.; Tikhe, J.; Ford, C. E.; Meador, J. W.; Ferre, R. A.; Brown, E. L.; Binford, S. L.; Brothers, M. A.; DeLisle, D. M.; Worland, S. T. Structure-assisted design of mechanism-based irreversible inhibitors of human rhinovirus 3C protease with potent antiviral activity against multiple rhinovirus serotypes. *Proc. Natl. Acad. Sci. U.S.A.* **1999**, *96*, 11000–11007.
- AG-7088 (rupintrivir) contains a Michael system (vinyl-Gln mimetic) as electrophile. It is in clinical development as an inhibitor of 3C proteases of human rhinoviruses. It is reported to exhibit low affinity to the SARS-CoV protease.¹⁷
- Schirmeister, T.; Klockow, A. Cysteine protease inhibitors containing small rings. *Mini-Rev. Med. Chem.* **2003**, *3*, 585–596.
- Powers, J. C.; Asgian, J. L.; Ekici, O. D.; James, K. E. Irreversible inhibitors of serine, cysteine, and threonine proteases. *Chem. Rev.* **2002**, *102*, 4639–4750.
- Ro, S.; Baek, S. G.; Lee, B.; Ok, J. H. Conformational studies of irreversible HIV-1 protease inhibitors containing *cis*-epoxide as an amide isostere. *J. Pept. Res.* **1999**, *54*, 242–248.
- Sprague, J. M. Diuretics. *Top. Med. Chem.* **1986**, *2*, 1–63.
- Kaeppler, U.; Schirmeister, T. New nonpeptidic inhibitors of papain derived from etacrynic acid. *Med. Chem.* **2005**, *1*, 361–370.
- Martina, E.; Stiefl, N.; Degel, B.; Schulz, F.; Breuning, A.; Schiller, M.; Vicik, R.; Baumann, K.; Ziebuhr, J.; Schirmeister, T. Screening of electrophilic compounds yields an aziridinyl peptide as new active-site directed SARS CoV main protease inhibitor. *Bioorg. Med. Chem. Lett.* **2005**, in press.
- Ziebuhr, J.; Heusipp, G.; Siddell, S. G. Biosynthesis, purification, and characterization of the human 229E 3C-like proteinase. *J. Virol.* **1997**, *71*, 3992–3997.
- Hegyvi, A.; Ziebuhr, J. Conservation of substrate specificities among coronavirus main proteases. *J. Gen. Virol.* **2002**, *83*, 595–599.
- The first peptide substrate VSYGSTLQ|AGLRKMA represents an HCoV-229E M^{pro} cleavage site.³⁶ The second peptide VSVNSTLQ|SGLRKMA was also shown to be cleaved effectively by SARS-CoV M^{pro} and, for this reason, is now being sold by Bachem as an SARS-CoV M^{pro} substrate (although it does not represent a cognate SARS-CoV M^{pro} cleavage site). The lower enzyme activity against this substrate is reflected in the higher incubation time used in the HPLC-based assays.
- FlexX*, version 1.12; BioSolveIT (An der Ziegelei 75, 53757): St. Augustin, Germany, 2003.

- (40) In some of the docking poses the studied compounds were not located within the binding site but were docked to the surface of the protein. Consequently, the "best" docking pose in this study was defined as the pose with the most favorable docking score for compounds that were located inside the binding pocket. For all virtual compounds (i.e., those that were not readily synthesized when the docking study was carried out) a further constraint was added. Since the activated double bond of compound **6a** was predicted to be in proximity to the active site Cys145 and since it was the working hypothesis that this double bond reacts with Cys145, only those docking poses were scrutinized where the double bond was close to Cys145.
- (41) His163 N-H \leftrightarrow O=C: 1.76 Å, angle NHO 153.1. Glu166 C=O \leftrightarrow H-N: 1.97 Å, angle NHO 169.3. Gln189 N-H \leftrightarrow O=C: 1.94 Å, angle NHO 141.1.
- (42) Adding the van der Waals radii of the involved heavy atoms sulfur and carbon results in 3.4 Å. Hence, when only noncovalent interactions are modeled, the two atoms cannot move closer because clashes are penalized by the scoring function of the docking tool.
- (43) Glu166 C=O \leftrightarrow H-N: 1.66 Å, angle NHO 159.5. Gln189 N-H \leftrightarrow O=C: 2.03 Å, angle NHO 170.2.
- (44) Thr190 C=O \leftrightarrow H-N: 1.70 Å, angle NHO 147.6. Gln192 N-H \leftrightarrow O=C: 2.03 Å, angle NHO 147.0.
- (45) Wang, Q. M.; Johnson, R. B.; Sommergruber, W.; Shepherd, T. A. Development of in vitro peptide substrates for human rhinovirus-12 2A protease. *Arch. Biochem. Biophys.* **1998**, *356*, 12–18.
- (46) The descriptors ortho and meta are used with respect to the phenolic hydroxyl group.
- (47) Rang, H. P.; Dale, M. M.; Ritter, J. M.; Moore, P. K. *Pharmacology*, 5th ed.; Churchill Livingstone: Edinburgh, U.K., 2003; p 362.
- (48) Hasannejad, H.; Takeda, M.; Taki, K.; Shin, H. J.; Babu, E.; Jutabha, P.; Khamdang, S.; Aleboyeh, M.; Onozato, M. L.; Tojo, A.; Enomoto, A.; Anzai, N.; Narikawa, S.; Huang, X.-L.; Niwa, T.; Endou, H. Interactions of human organic anion transporters with diuretics. *J. Pharmacol. Exp. Ther.* **2004**, *308*, 1021–1029.
- (49) Thiel, V.; Ivanov, K. A.; Putics, A.; Hertzog, T.; Schelle, B.; Bayer, S.; Weissbrich, B.; Snijder, E. J.; Rabenau, H.; Doerr, H. W.; Gorbalenya, A. E.; Ziebuhr, J. Mechanisms and enzymes involved in SARS coronavirus genome expression. *J. Gen. Virol.* **2003**, *84*, 2305–2315.
- (50) Liu, Y. Y.; Kati, W.; Chen, C. M.; Tripathi, R.; Molla, A.; Kohlbrenner, W. Use of a fluorescence plate reader for measuring kinetic parameters with inner filter effect correction. *Anal. Biochem.* **1999**, *267*, 331–335.
- (51) Since no time-dependent inhibition was observed with the tested compounds, only K_i values could be determined. Dialysis assays with the CAC1 cysteine protease cathepsin B showed the inhibitors to act reversibly (unpublished results).
- (52) *GraFit*; Erithacus Software Ltd.: London, 1994.
- (53) Diago-Meseguer, J.; Palomo-Coll, A. L.; Fernandez-Lizarbe, J. R.; Zugaza-Bilbao, A. A new reagent for activating carboxyl groups: preparation and reactions of *N,N*-bis[2-oxo-3-oxazolidinyl]phosphorodiamidic chloride. *Synthesis* **1980**, 547–551.
- (54) Robertson, A. Experiments on the synthesis of rotenone and its derivatives. Part II. The synthesis of rissic acid and of derric acid, and the constitution of rotenone, deguelin, and tephrosin. *J. Chem. Soc., Abstr.* **1932**, 1380–1388.
- (55) Coulthard, C. E.; Marshall, J.; Payman, F. L. The variation of phenol coefficients in homologous series of phenols. *J. Chem. Soc., Abstr.* **1930**, 280–291.
- (56) Buu-Hoi, N. P.; Xuong, N. D.; Lavit, D. Halogenated *o*- and *p*-phenolic ketones. *J. Chem. Soc.* **1954**, 1034–1038.
- (57) Nguyen, H.; Buu, H. Ketones derived from *o*-halogenated anisoles and phenetoles. *C. R. Hebd. Seances Acad. Sci.* **1947**, *224*, 1363.
- (58) Pinchuk, A. M.; Kosinskaya, I. M.; Shevchenko, V. I. *N*-(Cyanoalkyl)- and *N*-(cyanocycloalkyl)phosphorimidic trichlorides. *Zh. Obshch. Khim.* **1967**, *37*, 856–859.
- (59) Ziegler, E.; Schredt, H.; Gitschthaler, K. Synthesis of benzofulvenes. *Monatsh. Chem.* **1954**, *85*, 1234–1239.
- (60) Feniak, G.; Reckhow, W. A. Procède de photographie en couleurs et nouveaux produits pour sa mise en oeuvre (Procedure for color photography and new products for its implementation). Patent BE 560859, **1957** (Eastman Kodak Co.).
- (61) Pawar, R. A.; Shingte, R. D.; Gogte, V. N. Synthesis of potential plant growth regulators. Synthesis of 2-*N*-alkyl-5-chlorophenoxyacetic acids. *Indian J. Chem.* **1970**, *8*, 522–525.
- (62) SYBYL, version 6.9; Tripos Inc. (1699 South Hanley Road, St. Louis, MO 63144), 2001.
- (63) Yang, H.; Xie, W.; Xue, X.; Yang, K.; Ma, J.; Liang, W.; Zhao, Q.; Zhou, Z.; Pei, D.; Ziebuhr, J.; Hilgenfeld, R.; Yuen, K. Y.; Wong, L.; Gao, G.; Chen, S.; Chen, Z.; Ma, D.; Bartlam, M.; Rao, Z. Design of wide-spectrum inhibitors targeting coronavirus main proteases. *PLOS Biol.* **2005**, *3*, (10).

JM0501782